

# Metastability in Interacting Nonlinear Stochastic Differential Equations II: Large- $N$ Behaviour

Nils Berglund, Bastien Fernandez and Barbara Gentz

## Abstract

We consider the dynamics of a periodic chain of  $N$  coupled overdamped particles under the influence of noise, in the limit of large  $N$ . Each particle is subjected to a bistable local potential, to a linear coupling with its nearest neighbours, and to an independent source of white noise. For strong coupling (of the order  $N^2$ ), the system synchronises, in the sense that all particles assume almost the same position in their respective local potential most of the time. In a previous work, we showed that the transition from strong to weak coupling involves a sequence of symmetry-breaking bifurcations of the system's stationary configurations. We analysed, for arbitrary  $N$ , the behaviour for coupling intensities slightly below the synchronisation threshold. Here we describe the behaviour for any positive coupling intensity  $\gamma$  of order  $N^2$ , provided the particle number  $N$  is sufficiently large (as a function of  $\gamma/N^2$ ). In particular, we determine the transition time between synchronised states, as well as the shape of the “critical droplet” to leading order in  $1/N$ . Our techniques involve the control of the exact number of periodic orbits of a near-integrable twist map, allowing us to give a detailed description of the system's potential landscape, in which the metastable behaviour is encoded.

*Date.* November 21, 2006. Revised version, July 5, 2007.

*2000 Mathematical Subject Classification.* 37H20, 37L60 (primary), 37G40, 60K35 (secondary)

*Keywords and phrases.* Spatially extended systems, lattice dynamical systems, open systems, stochastic differential equations, interacting diffusions, Ginzburg–Landau SPDE, transitions times, most probable transition paths, large deviations, Wentzell-Freidlin theory, diffusive coupling, synchronisation, metastability, symmetry groups, symplectic twist maps.

## 1 Introduction

In this paper, we continue our analysis of the metastable dynamics of a periodic chain of coupled bistable elements, initiated in [BFG06a]. In contrast with similar models involving discrete on-site variables, or “spins”, whose metastable behaviour has been studied extensively (see for instance [dH04, OV05]), our model involves continuous local variables, and is therefore described by a set of interacting stochastic differential equations.

The analysis of the metastable dynamics of such a system requires an understanding of its  $N$ -dimensional “potential landscape”, in particular the number and location of its local minima and saddles of index 1. In [BFG06a], we showed that the number of stationary configurations increases from 3 to  $3^N$  as the coupling intensity  $\gamma$  decreases from a critical value  $\gamma_1$  of order  $N^2$  to 0. This transition from strong to weak coupling involves a sequence

of successive symmetry-breaking bifurcations, and we analysed in detail the first of these bifurcations, which corresponds to desynchronisation.

In the present work, we consider in more detail the behaviour for large particle number  $N$ . In the limit  $N \rightarrow \infty$ , the system tends to a Ginzburg–Landau stochastic partial differential equation (SPDE), studied for instance in [EH01, Rou02]. The Ginzburg–Landau SPDE describes in particular the behaviour near bifurcation points of more complicated equations, such as the stochastic Swift–Hohenberg equation [BHP05]. For large but finite  $N$ , it turns out that a technique known as “spatial map” analysis allows us to obtain a precise control of the set of stationary points, for values of the coupling well below the synchronisation threshold. More precisely, given a strictly positive coupling intensity  $\gamma$  of order  $N^2$ , there is an integer  $N_0(\gamma/N^2)$  such that for all  $N \geq N_0(\gamma/N^2)$ , we know precisely the number, location and type of the potential’s stationary points. This allows us to characterise the transition times and paths between metastable states for all these values of  $\gamma$  and  $N$ .

This paper is organised as follows. Section 2 contains the precise definition of our model, and the statement of all results. After introducing the model in Section 2.1 and describing general properties of the potential landscape in Section 2.2, we explain the heuristics for the limit  $N \rightarrow \infty$  in Section 2.3. In Section 2.4, we state the detailed results on number and location of stationary points for large but finite  $N$ , and in Section 2.5 we present their consequences for the stochastic dynamics. Section 3 contains the proofs of these results. The proofs rely on a detailed analysis of the orbits of period  $N$  of a near-integrable twist map, which are in one-to-one correspondence with stationary points of the potential. Appendix A recalls some properties of Jacobi’s elliptic functions needed in the analysis, while Appendix B contains some more technical proofs of results stated in Section 3.6.

## Acknowledgements

Financial support by the French Ministry of Research, by way of the *Action Concertée Incitative (ACI) Jeunes Chercheurs, Modélisation stochastique de systèmes hors équilibre*, is gratefully acknowledged. NB and BF thank the Weierstrass Institute for Applied Analysis and Stochastics (WIAS), Berlin, for financial support and hospitality. BG thanks the ESF Programme *Phase Transitions and Fluctuation Phenomena for Random Dynamics in Spatially Extended Systems (RDSES)* for financial support, and the Centre de Physique Théorique (CPT), Marseille, for kind hospitality.

## 2 Model and Results

### 2.1 Definition of the Model

Our model of interacting bistable systems perturbed by noise is defined by the following ingredients:

- The periodic one-dimensional lattice is given by  $\Lambda = \mathbb{Z}/N\mathbb{Z}$ , where  $N \geq 2$  is the number of particles.
- To each site  $i \in \Lambda$ , we attach a real variable  $x_i \in \mathbb{R}$ , describing the position of the  $i$ th particle. The configuration space is thus  $\mathcal{X} = \mathbb{R}^\Lambda$ .

- Each particle feels a local bistable potential, given by

$$U(\xi) = \frac{1}{4}\xi^4 - \frac{1}{2}\xi^2, \quad \xi \in \mathbb{R}. \quad (2.1)$$

The local dynamics thus tends to push the particle towards one of the two stable positions  $\xi = 1$  or  $\xi = -1$ .

- Neighbouring particles in  $\Lambda$  are coupled via a discretised-Laplacian interaction, of intensity  $\gamma/2$ .
- Each site is coupled to an independent source of noise, of intensity  $\sigma$ . The sources of noise are described by independent Brownian motions  $\{B_i(t)\}_{t \geq 0}$ .

The system is thus described by the following set of coupled stochastic differential equations, defining a diffusion on  $\mathcal{X}$ :

$$dx_i^\sigma(t) = f(x_i^\sigma(t)) dt + \frac{\gamma}{2} [x_{i+1}^\sigma(t) - 2x_i^\sigma(t) + x_{i-1}^\sigma(t)] dt + \sigma dB_i(t), \quad i \in \Lambda, \quad (2.2)$$

where the local nonlinear drift is given by

$$f(\xi) = -\nabla U(\xi) = \xi - \xi^3. \quad (2.3)$$

For  $\sigma = 0$ , the system (2.2) is a gradient system of the form  $\dot{x} = -\nabla V_\gamma(x)$ , with potential

$$V_\gamma(x) = \sum_{i \in \Lambda} U(x_i) + \frac{\gamma}{4} \sum_{i \in \Lambda} (x_{i+1} - x_i)^2. \quad (2.4)$$

## 2.2 Potential Landscape and Metastability

The dynamics of the stochastic system depends essentially on the “potential landscape”  $V_\gamma$ . As in [BFG06a], we use the notations

$$\mathcal{S} = \mathcal{S}(\gamma) = \{x \in \mathcal{X} : \nabla V_\gamma(x) = 0\} \quad (2.5)$$

for the set of stationary points, and  $S_k(\gamma)$  for the set of  $k$ -saddles, that is, stationary points with  $k$  unstable directions and  $N - k$  stable directions.

Understanding the dynamics for small noise essentially requires knowing the graph  $\mathcal{G} = (\mathcal{S}_0, \mathcal{E})$ , in which two vertices  $x^*, y^* \in \mathcal{S}_0$  are connected by an edge  $e \in \mathcal{E}$  if and only if there is a 1-saddle  $s \in \mathcal{S}_1$  whose unstable manifolds converge to  $x^*$  and  $y^*$ . The system behaves essentially like a Markovian jump process on  $\mathcal{G}$ . The mean transition time from  $x^*$  to  $y^*$  is of order  $e^{2H/\sigma^2}$ , where  $H$  is the potential difference between  $x^*$  and the lowest saddle leading to  $y^*$  (see [FW98]).

It is easy to see that  $\mathcal{S}$  always contains at least the three points

$$O = (0, \dots, 0), \quad I^\pm = \pm(1, \dots, 1). \quad (2.6)$$

Depending on the value of  $\gamma$ , the origin  $O$  can be an  $N$ -saddle, or a  $k$ -saddle for any odd  $k$ . The points  $I^\pm$  always belong to  $\mathcal{S}_0$ , in fact we have

$$V_\gamma(x) > V_\gamma(I^+) = V_\gamma(I^-) = -\frac{N}{4} \quad \forall x \in \mathcal{X} \setminus \{I^-, I^+\} \quad (2.7)$$

for all  $\gamma > 0$ , so that  $I^+$  and  $I^-$  represent the most stable configurations of the system. The three points  $O$ ,  $I^+$  and  $I^-$  are the only stationary points belonging to the diagonal

$$\mathcal{D} = \{x \in \mathcal{X} : x_1 = x_2 = \dots = x_N\}. \quad (2.8)$$

$N$	$x$	Type of symmetry
$4L$	$A$	$(x_1, \dots, x_L, x_L, \dots, x_1, -x_1, \dots, -x_L, -x_L, \dots, -x_1)$
	$B$	$(x_1, \dots, x_L, \dots, x_1, 0, -x_1, \dots, -x_L, \dots, -x_1, 0)$
$4L + 2$	$A$	$(x_1, \dots, x_{L+1}, \dots, x_1, -x_1, \dots, -x_{L+1}, \dots, -x_1)$
	$B$	$(x_1, \dots, x_L, x_L, \dots, x_1, 0, -x_1, \dots, -x_L, -x_L, \dots, -x_1, 0)$
$2L + 1$	$A$	$(x_1, \dots, x_L, -x_L, \dots, -x_1, 0)$
	$B$	$(x_1, \dots, x_L, x_L, \dots, x_1, x_0)$

TABLE 1. Symmetries of the stationary points bifurcating from the origin at  $\gamma = \gamma_1$ . The situation depends on whether  $N$  is odd (in which case we write  $N = 2L + 1$ ) or even (in which case we write  $N = 4L$  or  $N = 4L + 2$ , depending on the value of  $N \pmod{4}$ ). Points labelled  $A$  are 1-saddles near the desynchronisation bifurcation at  $\gamma = \gamma_1$ , those labelled  $B$  are 2-saddles (for odd  $N$ , this is actually a conjecture). More saddles of the same index are obtained by applying elements of the symmetry group  $G_N$  to  $A$  and  $B$ .

On the other hand, being a polynomial of degree 4 in  $N$  variables, the potential  $V_\gamma$  can have up to  $3^N$  stationary points.

The potential  $V_\gamma(x)$ , as well as the sets  $S(\gamma)$  and  $S_k(\gamma)$ , are invariant under the transformation group  $G = G_N$  of order  $4N$  (4 if  $N = 2$ ), generated by the following three symmetries:

- the rotation around the diagonal given by  $R(x_1, \dots, x_N) = (x_2, \dots, x_N, x_1)$ ;
- the mirror symmetry  $S(x_1, \dots, x_N) = (x_N, \dots, x_1)$ ;
- the point symmetry  $C(x_1, \dots, x_N) = -(x_1, \dots, x_N)$ .

In [BFG06a], we proved the following results:

- There is a critical coupling intensity

$$\gamma_1 = \frac{1}{1 - \cos(2\pi/N)} \quad (2.9)$$

such that for all  $\gamma \geq \gamma_1$ , the set of stationary points  $\mathcal{S}$  consists of the three points  $O$  and  $I^\pm$  only. The graph  $\mathcal{G}$  has two vertices  $I^\pm$ , connected by a single edge.

- As  $\gamma$  decreases below  $\gamma_1$ , an even number of new stationary points bifurcate from the origin. Half of them are 1-saddles, while the others are 2-saddles. These points satisfy symmetries as shown in Table 1. The potential difference between  $I^\pm$  and the 1-saddles behaves like  $N(1/4 - (\gamma_1 - \gamma)^2/6)$  as  $\gamma \nearrow \gamma_1$ .
- New bifurcations of the origin occur for  $\gamma = \gamma_M = (1 - \cos(2\pi M/N))^{-1}$ , with  $2 \leq M \leq N/2$ , in which saddles of order higher than 2 are created.

The number of stationary points emerging from the origin at the desynchronisation bifurcation at  $\gamma = \gamma_1$  depends on the parity of  $N$ . If  $N$  is even, there are exactly  $2N$  new points ( $N$  saddles of index 1, and  $N$  saddles of index 2). If  $N$  is odd, we were only able to prove that the number of new stationary points is a multiple of  $4N$ , but formulated the conjecture that there are exactly  $4N$  stationary points ( $2N$  saddles of index 1, and  $2N$  saddles of index 2). We checked this conjecture numerically for all  $N$  up to 101. As we shall see in Section 2.4, the conjecture is also true for  $N$  sufficiently large.

### 2.3 Heuristics for the Large- $N$ Limit

We want to determine the structure of the set  $\mathcal{S}$  of stationary points for large particle number  $N$ , and large coupling intensity  $\gamma$ . For this purpose, we introduce the rescaled coupling intensity

$$\tilde{\gamma} = \frac{\gamma}{\gamma_1} = \frac{2\pi^2}{N^2} \gamma \left[ 1 + \mathcal{O}\left(\frac{1}{N^2}\right) \right]. \quad (2.10)$$

Then, the desynchronisation bifurcation occurs for  $\tilde{\gamma} = 1$ . We will consider values of  $\tilde{\gamma}$  which may be smaller than 1, but are bounded away from zero. The reason why the set of stationary points can be controlled in this regime is that as  $N \rightarrow \infty$ , the deterministic system  $\dot{x} = -\nabla V_\gamma(x)$  behaves like a Ginzburg–Landau partial differential equation (PDE). Indeed, assume that the  $N$  sites of the chain are evenly distributed on a circle of radius 1, and that there exists a smooth function  $u(\varphi, t)$ ,  $\varphi \in \mathbb{S}^1$ , interpolating the coordinates of  $x(t)$  in such a way that

$$u\left(2\pi \frac{i}{N}, t\right) = x_i(t) \quad \forall i \in \Lambda. \quad (2.11)$$

Then in the limit  $N \rightarrow \infty$ , the discrete Laplacian in (2.2) converges to a constant times the second derivative of  $u(\cdot, t)$ , and we obtain the PDE

$$\partial_t u(\varphi, t) = f(u(\varphi, t)) + \tilde{\gamma} \partial_\varphi^2 u(\varphi, t). \quad (2.12)$$

Stationary solutions of (2.12) satisfy the equation

$$\tilde{\gamma} u''(\varphi) = -f(u(\varphi)), \quad (2.13)$$

describing the motion of a particle of mass  $\tilde{\gamma}$  in the *inverted* potential  $-U(\varphi)$ . The prefactor  $\tilde{\gamma}$  can be removed by scaling  $\varphi$ : Setting  $u_0(\phi) = u(\sqrt{\tilde{\gamma}}\phi)$ , we see that  $u_0$  satisfies the equation

$$u_0'' = -f(u_0) = u_0^3 - u_0. \quad (2.14)$$

All periodic solutions of this equation are known (cf. Section 3.3), and can be expressed in terms of Jacobi's elliptic functions<sup>1</sup> as

$$u_0(\phi) = a(\kappa) \operatorname{sn}\left(\frac{\phi - \phi_0}{\sqrt{1 + \kappa^2}}, \kappa\right), \quad (2.15)$$

where

- $\phi_0$  is an arbitrary phase;
- $\kappa \in [0, 1)$  is an auxiliary parameter controlling the shape of the function: For small  $\kappa$ , the function is close to a sine, while it approaches a square wave as  $\kappa \nearrow 1$ ;
- the amplitude  $a(\kappa)$  is given by

$$a(\kappa)^2 = \frac{2\kappa^2}{1 + \kappa^2}; \quad (2.16)$$

- the period of  $u_0(\varphi)$  is  $4\sqrt{1 + \kappa^2} K(\kappa)$ , where  $K$  denotes the complete elliptic integral of the first kind.

---

<sup>1</sup>For the reader's convenience, we recall the definitions and main properties of Jacobi's elliptic integrals and functions in Appendix A.

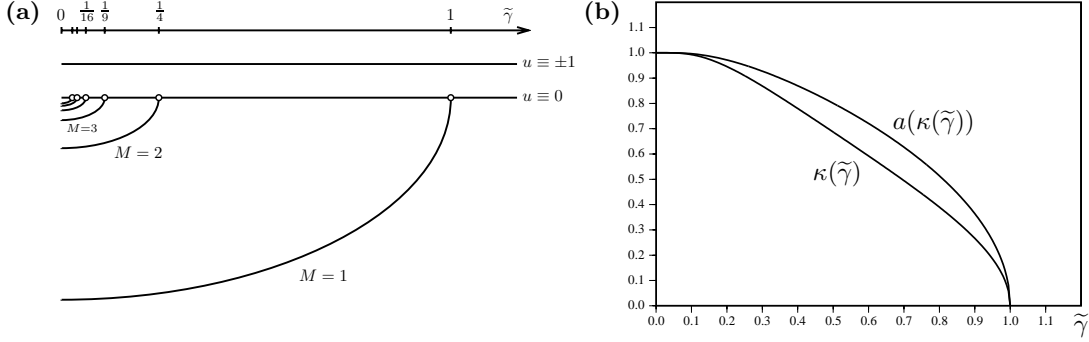


FIGURE 1. **(a)** Schematic bifurcation diagram of the limiting PDE (2.13). Whenever the rescaled coupling intensity  $\tilde{\gamma}$  decreases below  $1/M^2$ ,  $M = 1, 2, \dots$ , a one-parameter family of stationary solutions bifurcates from the identically zero solution  $u \equiv 0$ . **(b)** Relations between the shape parameter  $\kappa$ , the amplitude  $a$  and the rescaled coupling intensity  $\tilde{\gamma}$  for winding number  $M = 1$ .

We are looking for periodic solutions of (2.14) of period  $2\pi/\sqrt{\tilde{\gamma}}$ . Such solutions exist whenever the shape parameter  $\kappa$  satisfies the condition

$$4\sqrt{1+\kappa^2}K(\kappa) = \frac{2\pi M}{\sqrt{\tilde{\gamma}}} \quad (2.17)$$

for some integer  $M$ , which plays the rôle of a *winding number* controlling the number of sign changes of  $u_0$ . Equation (2.17) imposes a relation between shape parameter  $\kappa$  and rescaled coupling intensity  $\tilde{\gamma}$ , shown in Figure 1 in the case  $M = 1$ . On the other hand, the phase  $\phi_0$  is completely free.

The left-hand side of (2.17) being bounded below by  $2\pi$ , solutions of given winding number  $M$  exist provided  $\tilde{\gamma} \leq 1/M^2$ . The smaller  $\tilde{\gamma}$ , the more different types of periodic solutions exist. A new one-parameter family of stationary solutions, parametrised by  $\phi_0$ , bifurcates from the identically zero solution every time  $\tilde{\gamma}$  becomes smaller than  $1/M^2$ ,  $M = 1, 2, \dots$  (Figure 1a).

Finally, note that for stationary points  $x$  satisfying (2.11), with  $u$  given by (2.15), the value of the renormalised potential  $V_\gamma(x)/N$  converges, in the limit  $N \rightarrow \infty$ , to an integral which can be computed explicitly (see Section 3.3) in terms of the parameter  $\kappa$ :

$$\lim_{N \rightarrow \infty} \frac{V_\gamma(x)}{N} = -\frac{1}{3(1+\kappa^2)} \left[ \frac{2+\kappa^2}{1+\kappa^2} - 2 \frac{E(\kappa)}{K(\kappa)} \right], \quad (2.18)$$

where  $E$  denotes the complete elliptic integral of the second kind.

If we were to add noise to the PDE (2.12), we would obtain a Ginzburg–Landau SPDE. In that case, we expect that the configurations of highest energy reached in the course of a typical transition from  $u \equiv -1$  to  $u \equiv 1$  are of the form (2.15), with winding number  $M = 1$ . As a consequence, the potential difference in (2.18) should be governing the typical time of such transitions. However, proving this would involve an infinite-dimensional version of Wentzell–Freidlin theory, moreover in a degenerate situation, which is beyond the scope of the present work. We will henceforth consider situations with large, but finite particle number.

## 2.4 Main Results: Stationary Points for Large but Finite $N$

We examine now the structure of the set  $\mathcal{S}(\gamma)$  for large, but finite particle number  $N$ . Instead of the limiting differential equation (2.13), stationary points satisfy the difference equation

$$\frac{\gamma}{2}[x_{n+1} - 2x_n + x_{n-1}] = -f(x_n), \quad n \in \Lambda. \quad (2.19)$$

The key idea of the analysis is to interpret  $n$  as discrete time, and to consider (2.19) as defining  $x_{n+1}$  in terms of  $x_n$  and  $x_{n-1}$ . Setting  $v_n = x_n - x_{n-1}$  allows to rewrite (2.19) as the system

$$\begin{aligned} x_{n+1} &= x_n + v_{n+1}, \\ v_{n+1} &= v_n - 2\gamma^{-1}f(x_n). \end{aligned} \quad (2.20)$$

The map  $(x_n, v_n) \mapsto (x_{n+1}, v_{n+1})$  is an area-preserving twist map (“twist” meaning that  $x_{n+1}$  is a monotonous function of  $v_n$ ), for the study of which many tools are available [Mei92]. Stationary points of the potential  $V_\gamma$  are in one-to-one correspondence with periodic points of period  $N$  of this map. If we further scale  $v$  by a factor  $\varepsilon = \sqrt{2/\gamma}$ , we obtain the equivalent map

$$\begin{aligned} x_{n+1} &= x_n + \varepsilon y_{n+1}, \\ y_{n+1} &= y_n - \varepsilon f(x_n). \end{aligned} \quad (2.21)$$

The regime of large particle number  $N$  and finite rescaled coupling intensity  $\tilde{\gamma}$  corresponds to large  $\gamma$ , and thus to small  $\varepsilon$ . The map (2.21) is a discretisation of the system of ordinary differential equations  $\dot{x} = y$ ,  $\dot{y} = -f(x)$ , which is equivalent to the continuous limit equation (2.14). There should thus be some similarity between the orbits of the map (2.21) and of the system (2.14). In particular, one easily checks that the energy

$$E(x, \dot{x}) = \frac{1}{2}\dot{x}^2 - U(x), \quad (2.22)$$

which is conserved in the continuous limit, changes only slightly, by an amount of order  $\varepsilon^2$ , for the map (2.21) (setting  $y = \dot{x}$ ). The map is thus close to integrable, which makes its analysis accessible to perturbation theory.

Our main result, obtained by analysing the map (2.21), is that the bifurcation diagram looks like the one shown in Figure 2. Namely,

- For  $\tilde{\gamma} > 1$ ,  $I^+$ ,  $I^-$  and  $O$  are the only stationary points.
- Below  $\tilde{\gamma} = 1$ , an explicitly known number of saddles of index 1 and 2 bifurcate from the origin.
- For any  $2 \leq M \leq N/2$ , an explicitly known number of saddles of index  $2M - 1$  and  $2M$  bifurcate from the origin at  $\tilde{\gamma} = \tilde{\gamma}_M$ , where

$$\tilde{\gamma}_M = \frac{\gamma_M}{\gamma_1} = \frac{1 - \cos(2\pi/N)}{1 - \cos(2\pi M/N)} = \frac{1}{M^2} + \mathcal{O}\left(\frac{1}{N^2}\right). \quad (2.23)$$

- For any fixed  $M$ , if  $N$  is sufficiently large compared to  $M$ , the above list of stationary points is complete for  $\tilde{\gamma} > \tilde{\gamma}_M$ . In particular, there are no secondary bifurcations of existing branches of stationary points, and no stationary points created by saddle–node bifurcation for these values of  $\tilde{\gamma}$ .

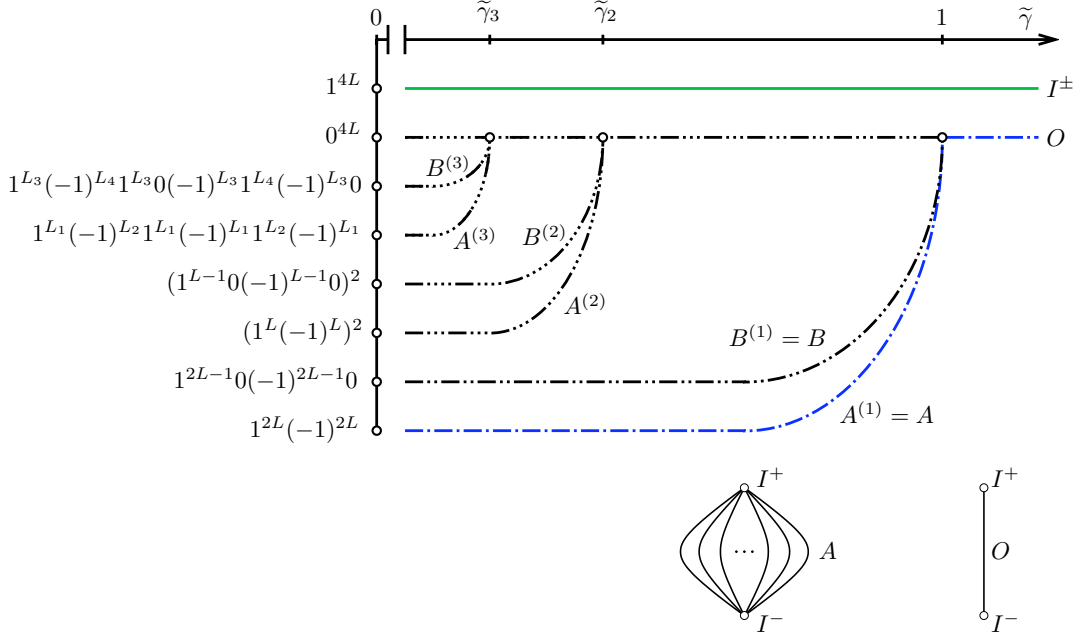


FIGURE 2. Partial bifurcation diagram for a case where  $N = 4L$  is a multiple of four, and some associated graphs  $\mathcal{G}$ . Only one stationary point per orbit of the symmetry group  $G$  is shown. Dash-dotted curves with  $k$  dots represent  $k$ -saddles. The symbols at the left indicate the zero-coupling limit of the stationary points' coordinates, for instance  $1^{2L}(-1)^{2L}$  stands for a point whose first  $2L$  coordinates are equal to 1, and whose last  $2L$  coordinates are equal to  $-1$ . The numbers associated with the branch created at  $\tilde{\gamma}_3$  are  $L_1 = \lfloor 2L/3 \rfloor$ ,  $L_2 = 2(L - L_1)$ ,  $L_3 = \lfloor 2L/3 + 1/2 \rfloor$  and  $L_4 = 2(L - L_3) - 1$  (in case  $N$  is a multiple of 12, there are more vanishing coordinates).

The main difficulty is to rule out the appearance of other stationary points away from the origin. Indeed, for perturbed integrable maps it is easy to obtain a lower bound on the number of periodic points, using the Poincaré–Birkhoff theorem, but it is hard to obtain an upper bound. One might imagine a scenario where stationary points appear far from the origin, which ultimately offer a more economic path for the transition from  $I^-$  to  $I^+$ .

We now give the precise formulation of the results. We first describe the behaviour between the first two bifurcation values  $\tilde{\gamma}_1$  and  $\tilde{\gamma}_2$ . Below,  $\gcd(a, b)$  denotes the greatest common divisor of two integers  $a$  and  $b$ , and  $O_x = \{gx : g \in G\}$  denotes the group orbit of a point  $x \in \mathcal{X}$  under the symmetry group  $G$ .

**Theorem 2.1.** *There exists  $N_1 < \infty$  such that when  $N \geq N_1$  and  $\tilde{\gamma}_2 < \tilde{\gamma} < \tilde{\gamma}_1 = 1$ , the set  $\mathcal{S}$  of stationary points of the potential  $V_\gamma$  has cardinality*

$$|\mathcal{S}| = 3 + \frac{4N}{\gcd(N, 2)} = \begin{cases} 3 + 2N & \text{if } N \text{ is even,} \\ 3 + 4N & \text{if } N \text{ is odd,} \end{cases} \quad (2.24)$$



There exist points  $A = A(\tilde{\gamma})$  and  $B = B(\tilde{\gamma})$  in  $\mathcal{X}$  such that  $\mathcal{S}$  can be decomposed as<sup>2</sup>

$$\begin{aligned}\mathcal{S}_0 &= O_{I^+} = \{I^+, I^-\}, \\ \mathcal{S}_1 &= O_A = \{\pm A, \pm RA, \dots, \pm R^{N-1}A\}, \\ \mathcal{S}_2 &= O_B = \{\pm B, \pm RB, \dots, \pm R^{N-1}B\}, \\ \mathcal{S}_3 &= O_O = \{O\}.\end{aligned}\tag{2.25}$$

The potential difference between the 1-saddles and the well bottoms (which is the same for all 1-saddles and well bottoms) satisfies

$$\frac{V_\gamma(A(\tilde{\gamma})) - V_\gamma(I^\pm)}{N} = \frac{1}{4} - \frac{1}{3(1 + \kappa^2)} \left[ \frac{2 + \kappa^2}{1 + \kappa^2} - 2 \frac{E(\kappa)}{K(\kappa)} \right] + \mathcal{O}\left(\frac{\kappa^2}{N}\right),\tag{2.26}$$

where  $\kappa = \kappa(\tilde{\gamma})$  is defined implicitly by

$$\tilde{\gamma} = \frac{\pi^2}{4K(\kappa)^2(1 + \kappa^2)}.\tag{2.27}$$

The detailed proofs are given in Section 3.

The second result, which is also proved in Section 3, concerns the behaviour for subsequent bifurcation values  $\tilde{\gamma}_M$ ,  $M \geq 2$ .

**Theorem 2.2.** *For any  $M \geq 2$ , there exists  $N_M < \infty$  such that when  $N \geq N_M$  and  $\tilde{\gamma}_{M+1} < \tilde{\gamma} < \tilde{\gamma}_M$ , the set  $\mathcal{S}$  of stationary points of the potential  $V_\gamma$  has cardinality*

$$|\mathcal{S}| = 3 + \sum_{m=1}^M \frac{4N}{\gcd(N, 2m)}.\tag{2.28}$$

There exist points  $A^{(m)}$  and  $B^{(m)}$  in  $\mathcal{X}$ ,  $m = 1, \dots, M$ , such that  $\mathcal{S}$  can be decomposed as

$$\begin{aligned}\mathcal{S}_0 &= O_{I^+} = \{I^+, I^-\}, \\ \mathcal{S}_{2m-1} &= O_{A^{(m)}}, & m = 1, \dots, M, \\ \mathcal{S}_{2m} &= O_{B^{(m)}}, & m = 1, \dots, M, \\ \mathcal{S}_{2M+1} &= O_O = \{O\},\end{aligned}\tag{2.29}$$

The potential difference between the saddles  $A_j^{(m)}(\tilde{\gamma})$  and the well bottoms satisfies a similar relation as (2.26), but with  $\kappa = \kappa(m^2\tilde{\gamma})$ .

**Remark 2.3.** The proof actually yields information on the coordinates of the points  $A = A(\tilde{\gamma})$  and  $B = B(\tilde{\gamma})$ :

- The coordinates of  $A$  and  $B$  satisfy the symmetries indicated in Table 1.
- If  $N$  is even, the coordinates of  $A$  and  $B$  are given by

$$\begin{aligned}A_j(\tilde{\gamma}) &= a(\kappa(\tilde{\gamma})) \operatorname{sn}\left(\frac{4K(\kappa(\tilde{\gamma}))}{N}\left(j - \frac{1}{2}\right), \kappa(\tilde{\gamma})\right) + \mathcal{O}\left(\frac{1}{N}\right), \\ B_j(\tilde{\gamma}) &= a(\kappa(\tilde{\gamma})) \operatorname{sn}\left(\frac{4K(\kappa(\tilde{\gamma}))}{N}j, \kappa(\tilde{\gamma})\right) + \mathcal{O}\left(\frac{1}{N}\right),\end{aligned}\tag{2.30}$$

where the amplitude  $a(\kappa)$  is the one defined in (2.16).

---

<sup>2</sup>If  $N$  is even, the orbits  $O_A$  and  $O_B$  contain  $N$  instead of  $2N$  points, because  $R^{N/2} = -\mathbb{1}$ .

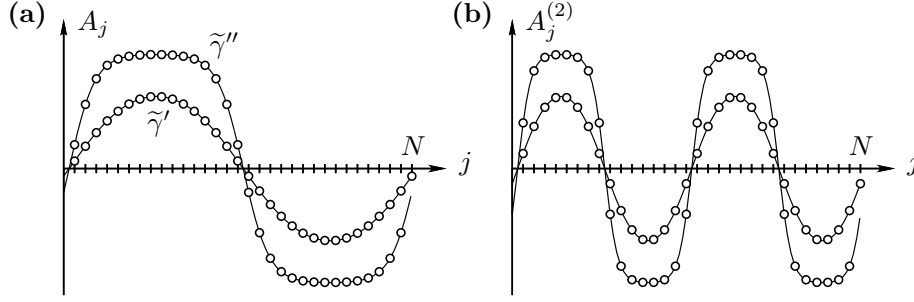


FIGURE 3. **(a)** Coordinates of the 1-saddles  $A$  in the case  $N = 32$ , shown for two different values of the coupling  $\tilde{\gamma}' > \tilde{\gamma}''$ . **(b)** Coordinates of the 3-saddles  $A^{(2)}$  in the case  $N = 32$ , shown for the coupling intensities  $\tilde{\gamma}'/4$  and  $\tilde{\gamma}''/4$ .

- If  $N$  is odd, the coordinates of  $A$  and  $B$  are given by

$$\begin{aligned} A_j(\tilde{\gamma}) &= a(\kappa(\tilde{\gamma})) \operatorname{sn}\left(\frac{4K(\kappa(\tilde{\gamma}))}{N}j, \kappa(\tilde{\gamma})\right) + \mathcal{O}\left(\frac{1}{N}\right), \\ B_j(\tilde{\gamma}) &= a(\kappa(\tilde{\gamma})) \operatorname{cn}\left(\frac{4K(\kappa(\tilde{\gamma}))}{N}j, \kappa(\tilde{\gamma})\right) + \mathcal{O}\left(\frac{1}{N}\right). \end{aligned} \quad (2.31)$$

- The components of  $A^{(m)}$  and  $B^{(m)}$  are given by similar expressions, with  $\tilde{\gamma}$  replaced by  $m^2\tilde{\gamma}$ ,  $j - \frac{1}{2}$  replaced by  $m(j - \frac{1}{2})$  and  $j$  replaced by  $mj$ .
- Note that the total number of stationary points accounted for by these results is of the order  $N^2$ , which is much less than the  $3^N$  points present at zero coupling. Many additional stationary points thus have to be created as the rescaled coupling intensity  $\tilde{\gamma}$  decreases sufficiently, either by pitchfork-type second-order bifurcations of already existing points, or by saddle-node bifurcations. However, the values  $\tilde{\gamma}(N)$  for which these bifurcations occur have to satisfy  $\lim_{N \rightarrow \infty} \tilde{\gamma}(N) = 0$ .

The existence of second-order bifurcations follows from stability arguments. For instance, for even  $N$ , the point  $A(\tilde{\gamma})$  converges to  $(1, 1, \dots, 1, -1, -1, \dots, -1)$  as  $\tilde{\gamma} \rightarrow 0$ , which is a local minimum of  $V_\gamma$  instead of a 1-saddle. The  $A$ -branch thus has to bifurcate at least once as the coupling decreases to zero (Figure 4). For odd  $N$ , by contrast, the point  $A(\tilde{\gamma})$  converges to  $(1, 1, \dots, 1, 0, -1, -1, \dots, -1)$  as  $\tilde{\gamma} \rightarrow 0$ , which is also a 1-saddle. We thus expect that the point  $A(\tilde{\gamma})$  does not undergo any bifurcations for  $0 \leq \tilde{\gamma} < 1$  if  $N$  is odd.

## 2.5 Stochastic Case

We return now to the behaviour of the system of stochastic differential equations

$$dx_i^\sigma(t) = f(x_i^\sigma(t)) dt + \frac{\gamma}{2} [x_{i+1}^\sigma(t) - 2x_i^\sigma(t) + x_{i-1}^\sigma(t)] dt + \sigma dB_i(t), \quad i \in \Lambda. \quad (2.32)$$

Our main goal is to characterise the noise-induced transition from the configuration  $I^- = (-1, -1, \dots, -1)$  to the configuration  $I^+ = (1, 1, \dots, 1)$ . In particular, we are interested in the time needed for this transition to occur, and by the shape of the critical configuration, i.e., the configuration of highest energy reached during the transition.

In [BFG06a, Theorem 2.7], we obtained that in the synchronisation regime  $\tilde{\gamma} > 1$ , for any initial condition  $x_0$  in a ball  $\mathcal{B}(I^-, r)$  of radius  $r < 1/2$  around  $I^-$ , any particle

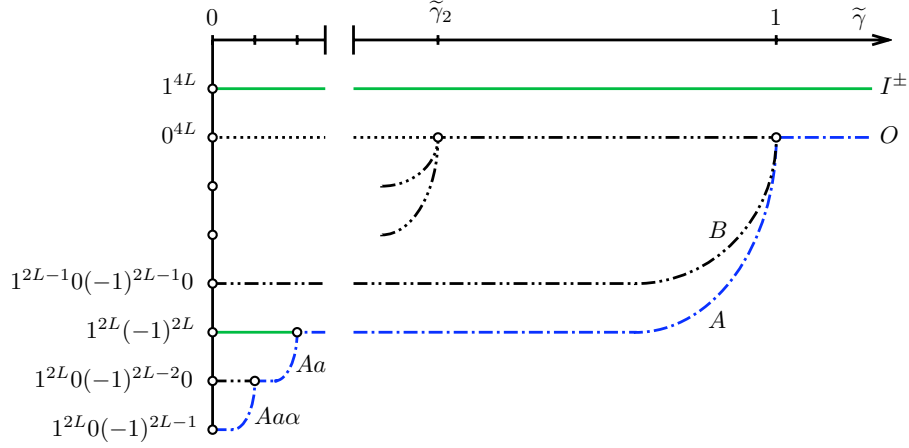


FIGURE 4. Partial bifurcation diagram for a case where  $N = 4L$  is a multiple of four, showing the expected bifurcation behaviour of the critical 1-saddle in the zero-coupling limit.

number  $N \geq 2$  and any constant  $\delta > 0$ , the first-hitting time  $\tau_+ = \tau^{\text{hit}}(\mathcal{B}(I_+, r))$  of a ball  $\mathcal{B}(I^+, r)$  of radius  $r$  around  $I^+$  satisfies

$$\lim_{\sigma \rightarrow 0} \mathbb{P}^{x_0} \{e^{(N/2-\delta)/\sigma^2} < \tau_+ < e^{(N/2+\delta)/\sigma^2}\} = 1 \quad (2.33)$$

and

$$\lim_{\sigma \rightarrow 0} \sigma^2 \log \mathbb{E}^{x_0} \{\tau_+\} = \frac{N}{2}. \quad (2.34)$$

This means that in the synchronisation regime, the transition between  $I^-$  and  $I^+$  takes a time of the order  $e^{N/2\sigma^2}$ . Furthermore, for any fixed radius  $R \in (r, 1/2)$ , the first-hitting time  $\tau_O = \tau^{\text{hit}}(\mathcal{B}(O, r))$  of a ball around the origin satisfies

$$\lim_{\sigma \rightarrow 0} \mathbb{P}^{x_0} \{\tau_O < \tau_+ \mid \tau_+ < \tau_-\} = 1, \quad (2.35)$$

where  $\tau_- = \inf\{t > \tau^{\text{exit}}(\mathcal{B}(I^-, R)) : x_t \in \mathcal{B}(I^-, r)\}$  is the time of first return to the small ball  $\mathcal{B}(I^-, r)$  after leaving the larger ball  $\mathcal{B}(I^-, R)$ . This means that during a transition, the system is likely to pass close to the origin, i.e., the origin, being the only saddle of  $V_\gamma$ , is the critical configuration of the transition.

We can now prove a similar result in the desynchronised regime  $\tilde{\gamma} < 1$ .

**Theorem 2.4.** *For  $\tilde{\gamma} < 1$ , let*

$$h(\tilde{\gamma}) = \frac{V_\gamma(A(\tilde{\gamma})) - V_\gamma(I^\pm)}{N} = \frac{1}{4} - \frac{1}{3(1+\kappa^2)} \left[ \frac{2+\kappa^2}{1+\kappa^2} - 2 \frac{E(\kappa)}{K(\kappa)} \right] + \mathcal{O}\left(\frac{\kappa^2}{N}\right), \quad (2.36)$$

where  $\kappa = \kappa(\tilde{\gamma})$  is defined implicitly by (2.27). Fix an initial condition  $x_0 \in \mathcal{B}(I^-, r)$ . Then for any  $0 < \tilde{\gamma} < 1$ , and any  $\delta > 0$ , there exists  $N_0(\tilde{\gamma})$  such that for all  $N > N_0(\tilde{\gamma})$ ,

$$\lim_{\sigma \rightarrow 0} \mathbb{P}^{x_0} \{e^{(2Nh(\tilde{\gamma})-\delta)/\sigma^2} < \tau_+ < e^{(2Nh(\tilde{\gamma})+\delta)/\sigma^2}\} = 1 \quad (2.37)$$

and

$$\lim_{\sigma \rightarrow 0} \sigma^2 \log \mathbb{E}^{x_0} \{\tau_+\} = 2Nh(\tilde{\gamma}). \quad (2.38)$$

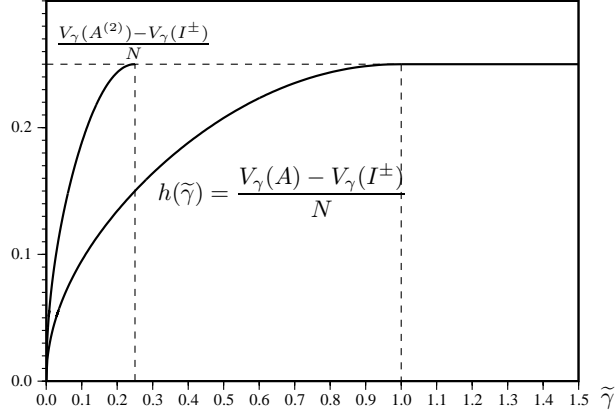


FIGURE 5. Value of the rescaled potential barrier height  $h(\tilde{\gamma}) = (V_\gamma(A) - V_\gamma(I^\pm))/N$  as a function of the rescaled coupling intensity  $\tilde{\gamma}$ . For comparison, we also show the rescaled barrier height  $(V_\gamma(A^{(2)}) - V_\gamma(I^\pm))/N$  for a stationary point of the higher winding number  $M = 2$ .

Furthermore, let

$$\tau_A = \tau^{\text{hit}} \left( \bigcup_{g \in G} \mathcal{B}(gA, r) \right), \quad (2.39)$$

where  $A = A(\tilde{\gamma})$  satisfies (2.30) (or (2.31) if  $N$  is odd). Then for any  $N > N_0(\tilde{\gamma})$ ,

$$\lim_{\sigma \rightarrow 0} \mathbb{P}^{x_0} \{ \tau_A < \tau_+ \mid \tau_+ < \tau_- \} = 1. \quad (2.40)$$

The relations (2.37) and (2.38) mean that the transition time between the synchronised states  $I^-$  and  $I^+$  is of order  $e^{2Nh(\tilde{\gamma})/\sigma^2}$ , while relation (2.40) implies that the set of critical configurations is given by the group orbit of  $A$  under  $G$ .

The large- $N$  limit of the rescaled potential difference  $h(\tilde{\gamma})$  is shown in Figure 5. The limiting function is increasing, with a discontinuous second-order derivative at  $\tilde{\gamma} = 1$ . For small  $\tilde{\gamma}$ ,  $h(\tilde{\gamma})$  grows like the square-root of  $\tilde{\gamma}$ . This is compatible with the weak-coupling behaviour  $h = (1/4 + 3/2\gamma + \mathcal{O}(\gamma^2))/N$  obtained in [BFG06a], if one takes into account the scaling of  $\tilde{\gamma}$ .

The critical configuration, that is, the configuration with highest energy reached in the course of the transition from  $I^-$  to  $I^+$ , is any translate of the configuration  $A(\tilde{\gamma})$  shown in Figure 3a. If  $N$  is even, it has  $N/2$  positive and  $N/2$  negative coordinates, while for odd  $N$ , there are  $(N-1)/2$  positive, one vanishing, and  $(N-1)/2$  negative coordinates. The sites with positive and negative coordinates are always adjacent. The potential difference between the 1-saddles  $A$  and the 2-saddles  $B$  is actually very small, so that transition paths become less localised as the particle number  $N$  increases, reflecting the fact that the system becomes translation-invariant in the large- $N$  limit.

### 3 Proofs

#### 3.1 Strategy of the Proof

The proof of Theorems 2.1 and 2.2 is based on the fact that stationary points of the potential satisfy the relation

$$f(x_n) + \frac{\gamma}{2}[x_{n+1} - 2x_n + x_{n-1}] = 0, \quad (3.1)$$

where  $f(x) = x - x^3$ . As mentioned in Section 2.4, this relation can be rewritten as a two-dimensional area-preserving twist map

$$\begin{aligned} x_{n+1} &= x_n + v_{n+1}, \\ v_{n+1} &= v_n - 2\gamma^{-1}f(x_n). \end{aligned} \quad (3.2)$$

whose periodic points correspond to stationary points of the potential. In fact, we are going to analyse a slightly different equivalent map, which has the advantage to use the symmetries of the model in a more efficient way.

The proof is organised as follows:

- In Section 3.2, we introduce the alternative twist map, adapted to symmetries.
- In Section 3.3, we compute the expression of the map in action–angle variables, taking advantage of the existence of an almost conserved quantity.
- In Section 3.4, we compute the generating function of the map in action–angle variables. This reduces the problem of finding periodic orbits to a variational problem (which is simpler than the original one).
- The main difficulty is that the system is almost degenerate along the translation mode. In Section 3.5, we introduce Fourier variables in order to decouple the translation mode from the other, “oscillating” modes.
- In Section 3.6, we deal with the oscillating modes, by showing with the help of Banach’s contraction principle that for each value of the translation mode, there is exactly one value of the oscillating modes yielding a stationary point.
- In Section 3.7, we deal with the translation mode, by reducing the problem to one dimension, and showing that the generating function is dominated by its leading Fourier mode in this direction. This yields the exact number of stationary points.
- Finally, in Section 3.8 we consider the stability of the stationary points.

#### 3.2 Symmetric Twist Map

The twist map (3.2) does not exploit the symmetries of the original system in an optimal way. In order to do so, it is more advantageous to introduce the variable

$$u_n = \frac{x_{n+1} - x_{n-1}}{2} \quad (3.3)$$

instead of  $v_n$ . Then a short computation shows that

$$\begin{aligned} x_{n+1} &= x_n + u_n - \gamma^{-1}f(x_n), \\ u_{n+1} &= u_n - \gamma^{-1}[f(x_n) + f(x_{n+1})]. \end{aligned} \quad (3.4)$$

The map  $T_1 : (x_n, u_n) \mapsto (x_{n+1}, u_{n+1})$  is also an area-preserving twist map. Although it looks more complicated than the map (3.2), it has the advantage that its inverse is

obtained by changing the sign of  $u$ , namely

$$\begin{aligned} x_n &= x_{n+1} - u_{n+1} - \gamma^{-1} f(x_{n+1}) , \\ u_n &= u_{n+1} + \gamma^{-1} [f(x_{n+1}) + f(x_n)] . \end{aligned} \quad (3.5)$$

This implies that if we introduce the involutions

$$S_1 : (x, u) \mapsto (-x, u) \quad \text{and} \quad S_2 : (x, u) \mapsto (x, -u) , \quad (3.6)$$

then the map  $T_1$  and its inverse are related by

$$T_1 \circ S_1 = S_1 \circ (T_1)^{-1} \quad \text{and} \quad T_1 \circ S_2 = S_2 \circ (T_1)^{-1} , \quad (3.7)$$

as a consequence of  $f$  being odd. This implies that the images of an orbit of the map under  $S_1$  and  $S_2$  are also orbits of the map.

For large  $N$ , it turns out to be useful to introduce the small parameter

$$\varepsilon = \sqrt{\frac{2}{\gamma}} = \sqrt{\frac{2}{\gamma_1 \tilde{\gamma}}} = \frac{2\pi}{N\sqrt{\tilde{\gamma}}} \left( 1 + \mathcal{O}\left(\frac{1}{N^2}\right) \right) , \quad (3.8)$$

and the scaled variable  $w = u/\varepsilon$ . This transforms the map  $T_1$  into a map  $T_2 : (x_n, w_n) \mapsto (x_{n+1}, w_{n+1})$  defined by

$$\begin{aligned} x_{n+1} &= x_n + \varepsilon w_n - \frac{1}{2} \varepsilon^2 f(x_n) , \\ w_{n+1} &= w_n - \frac{1}{2} \varepsilon [f(x_n) + f(x_{n+1})] . \end{aligned} \quad (3.9)$$

$T_2$  is again an area-preserving twist map satisfying

$$T_2 \circ S_1 = S_1 \circ (T_2)^{-1} \quad \text{and} \quad T_2 \circ S_2 = S_2 \circ (T_2)^{-1} . \quad (3.10)$$

### 3.3 Action–Angle Variables

For small  $\varepsilon$ , we expect the orbits of this map to be close to those of the differential equation

$$\begin{aligned} \dot{x} &= w , \\ \dot{w} &= -f(x) , \end{aligned} \quad (3.11)$$

which is equivalent to the second-order equation  $\ddot{x} = -f(x)$  describing the motion of a particle in the *inverted* double-well potential  $-U(x)$ , compare (2.14). Solutions of (3.11) can be expressed in terms of Jacobi elliptic functions. Indeed, the function

$$C(x, w) = \frac{1}{2}(x^2 + w^2) - \frac{1}{4}x^4 \quad (3.12)$$

being a constant of motion, one sees that  $w$  satisfies

$$w = \pm \sqrt{(a(C)^2 - x^2)(b(C)^2 - x^2)/2} , \quad (3.13)$$

where

$$\begin{aligned} a(C)^2 &= 1 - \sqrt{1 - 4C} , \\ b(C)^2 &= 1 + \sqrt{1 - 4C} . \end{aligned} \quad (3.14)$$

This can be used to integrate the equation  $\dot{x} = w$ , yielding

$$\frac{b(C)}{\sqrt{2}}t = F\left(\operatorname{Arcsin}\left(\frac{x(t)}{a(C)}\right), \kappa(C)\right), \quad (3.15)$$

where  $\kappa(C) = a(C)/b(C)$ , and  $F(\phi, \kappa)$  denotes the incomplete elliptic integral of the first kind. The solution of the ODE can be written in terms of standard elliptic functions as

$$\begin{aligned} x(t) &= a(C) \operatorname{sn}\left(\frac{b(C)}{\sqrt{2}}t, \kappa(C)\right), \\ w(t) &= \sqrt{2C} \operatorname{cn}\left(\frac{b(C)}{\sqrt{2}}t, \kappa(C)\right) \operatorname{dn}\left(\frac{b(C)}{\sqrt{2}}t, \kappa(C)\right). \end{aligned} \quad (3.16)$$

We return now to the map  $T_2$  defined in (3.9). The explicit solution of the continuous-time equation motivates the change of variables  $\Phi_1 : (x, w) \mapsto (\varphi, C)$  given by

$$\begin{aligned} \varphi &= \frac{\sqrt{2}}{b(C)} F\left(\operatorname{Arcsin}\left(\frac{x}{a(C)}\right), \kappa(C)\right), \\ C &= \frac{1}{2}(x^2 + w^2) - \frac{1}{4}x^4. \end{aligned} \quad (3.17)$$

One checks that  $\Phi_1$  is again area-preserving. The inverse  $\Phi_1^{-1}$  is given by

$$\begin{aligned} x &= a(C) \operatorname{sn}\left(\frac{b(C)}{\sqrt{2}}\varphi, \kappa(C)\right), \\ w &= \sqrt{2C} \operatorname{cn}\left(\frac{b(C)}{\sqrt{2}}\varphi, \kappa(C)\right) \operatorname{dn}\left(\frac{b(C)}{\sqrt{2}}\varphi, \kappa(C)\right). \end{aligned} \quad (3.18)$$

The elliptic functions  $\operatorname{sn}$ ,  $\operatorname{cn}$  and  $\operatorname{dn}$  being periodic in their first argument, with period  $4K(\kappa)$ , it is convenient to carry out a further area-preserving change of variables  $\Phi_2 : (\varphi, C) \mapsto (\psi, I)$ , defined by

$$\psi = \Omega(C)\varphi, \quad I = h(C), \quad (3.19)$$

where

$$\Omega(C) = \frac{b(C)}{\sqrt{2}} \frac{\pi}{2K(\kappa(C))}, \quad h(C) = \int_0^C \frac{dC'}{\Omega(C')}. \quad (3.20)$$

Using the facts that  $C$  and  $b = b(C)$  can be expressed as functions of  $\kappa = \kappa(C)$  by  $C = \kappa^2/(1 + \kappa^2)^2$  and  $b^2 = 2/(1 + \kappa^2)$ , one can check that

$$h(C) = \frac{4}{3\pi} \frac{(1 + \kappa^2)E(\kappa) - (1 - \kappa^2)K(\kappa)}{(1 + \kappa^2)^{3/2}} \Big|_{\kappa=\kappa(C)} \in \left[0, \frac{2\sqrt{2}}{3\pi}\right]. \quad (3.21)$$

We denote by  $\Phi = \Phi_2 \circ \Phi_1$  the transformation  $(x, w) \mapsto (\psi, I)$  and by  $T = \Phi \circ T_2 \circ \Phi^{-1}$  the resulting map.

**Proposition 3.1.** *The map  $T = T(\varepsilon)$  has the form*

$$\begin{aligned} \psi_{n+1} &= \psi_n + \varepsilon \overline{\Omega}(I_n) + \varepsilon^3 f(\psi_n, I_n, \varepsilon) \pmod{2\pi}, \\ I_{n+1} &= I_n + \varepsilon^3 g(\psi_n, I_n, \varepsilon), \end{aligned} \quad (3.22)$$

where  $\bar{\Omega}(I) = \Omega(h^{-1}(I))$ . The functions  $f$  and  $g$  are  $\pi$ -periodic in their first argument, and are real-analytic for  $0 \leq I \leq h(1/4) - \mathcal{O}(\varepsilon^3)$ . Furthermore,  $T$  satisfies the symmetries

$$T \circ \Sigma_1 = \Sigma_1 \circ T^{-1} \quad \text{and} \quad T \circ \Sigma_2 = \Sigma_2 \circ T^{-1}, \quad (3.23)$$

where  $\Sigma_1(\psi, I) = (-\psi, I)$  and  $\Sigma_2(\psi, I) = (\pi - \psi, I)$ .

PROOF: First observe that  $\Phi_1$  and  $\Phi$  are analytic whenever  $(x, w)$  is such that  $C < 1/4$ . The map  $T$  will thus be analytic whenever  $(\psi_n, I_n)$  is such that  $C(x_n, w_n) < 1/4$  and  $C(x_{n+1}, w_{n+1}) < 1/4$ . A direct computation shows that

$$C(x_{n+1}, w_{n+1}) - C(x_n, w_n) = \frac{\varepsilon^3}{4} \left[ x_n w_n + 2x_n w_n^3 - 4x_n^3 w_n + 3x_n^5 w_n \right] + \mathcal{O}(\varepsilon^4). \quad (3.24)$$

This implies that  $I_{n+1} = I_n + \mathcal{O}(\varepsilon^3)$ , and allows to determine  $g(\psi, I, 0)$ . It also shows that  $T$  is analytic for  $I_n < h(1/4) - \mathcal{O}(\varepsilon^3)$ . Furthermore, writing  $a_n = a(C(x_n, w_n))$ , we see that (3.24) implies  $a_{n+1} - a_n = \mathcal{O}(\varepsilon^3)$  and similarly for  $b_n, \kappa_n$ . This yields

$$\begin{aligned} \varphi(x_{n+1}, w_{n+1}) - \varphi(x_n, w_n) &= \frac{\sqrt{2}}{b_n} \int_{x_n/a_n}^{x_{n+1}/a_n} \frac{du}{\sqrt{(1 - \kappa_n^2 u^2)(1 - u^2)}} + \mathcal{O}(\varepsilon^3) \\ &= \varepsilon + \mathcal{O}(\varepsilon^3), \end{aligned} \quad (3.25)$$

which implies the expression for  $\psi_{n+1}$ . We remark that the fact that  $T$  is area-preserving implies the relation

$$1 = \frac{\partial(\psi_{n+1}, I_{n+1})}{\partial(\psi_n, I_n)} = 1 + \varepsilon^3 \left[ \partial_\psi f(\psi, I, 0) + \partial_I g(\psi, I, 0) \right] + \mathcal{O}(\varepsilon^4), \quad (3.26)$$

which allows to determine  $f(\psi, I, 0)$ . The fact that  $f$  and  $g$  are  $\pi$ -periodic in their first argument is a consequence of the fact that  $T_2(-x, -w) = -T_2(x, w)$ . Finally the relations (3.23) follow from the symmetries (3.10), with  $\Sigma_i = \Phi \circ S_i \circ \Phi^{-1}$ .  $\square$

A perturbation expansion at  $I = 0$  shows in particular that

$$\bar{\Omega}(I) = 1 - \frac{3}{4}I + \mathcal{O}(I^2). \quad (3.27)$$

An important observation is that  $\bar{\Omega}(I)$  is a monotonously decreasing function, taking values in  $[0, 1]$ . The monotonicity of  $\bar{\Omega}$  makes  $T$  a *twist map* for sufficiently small  $\varepsilon$ , which has several important consequences on existence of periodic orbits.

We call *rotation number* of a periodic orbit of period  $N$  the quantity

$$\nu = \frac{1}{2\pi N} \left[ \sum_{n=1}^N (\psi_{n+1} - \psi_n) \pmod{2\pi} \right]. \quad (3.28)$$

Note that because of periodicity,  $\nu$  is necessarily a rational number of the form  $\nu = M/N$ , for some positive integer  $M$ . We denote by  $\mathbb{T}_\nu^N$  the set of points  $\psi$  in the torus  $\mathbb{T}^N$  satisfying (3.28). It is sometimes more convenient to visualise  $\mathbb{T}_\nu^N$  as the set of real  $N$ -tuples  $(\psi_1, \dots, \psi_N)$  such that

$$\psi_1 < \psi_2 < \dots < \psi_N < \psi_1 + 2\pi N\nu. \quad (3.29)$$



In the sequel, we shall use the shorthand *stationary point with rotation number  $\nu$*  instead of *stationary point corresponding to a periodic orbit of rotation number  $\nu$* .

The expression (3.22) for  $T$  implies that

$$\nu = \frac{\bar{\Omega}(I_0)}{2\pi}\varepsilon + \mathcal{O}(\varepsilon^2). \quad (3.30)$$

The following properties follow from the Poincaré–Birkhoff theorem, whenever  $\varepsilon > 0$  is sufficiently small:

- For each positive integer  $M$  satisfying

$$M \leq \frac{N\varepsilon}{2\pi}(1 + \mathcal{O}(\varepsilon)), \quad (3.31)$$

the twist map  $T$  admits at least two periodic orbits of period  $N$  and rotation number  $\nu = M/N$ . Note that Condition (3.31) is compatible with the fact that  $O$  bifurcates for  $\gamma = \gamma_M$ ,  $M = 1, 2, \dots, \lfloor N/2 \rfloor$ .

- Any periodic orbit of period  $N$  of the map  $T$  is of the form

$$\begin{aligned} \psi_n &= \psi_0 + 2\pi\nu n + \mathcal{O}(\varepsilon^2), \\ I_n &= \bar{\Omega}^{-1}\left(\frac{2\pi}{\varepsilon}\nu\right) + \mathcal{O}(\varepsilon^2), \end{aligned} \quad (3.32)$$

for some  $\psi_0$  and some  $\nu = M/N$ , where  $M$  is a positive integer satisfying (3.31).

Going back to original variables, we see that these periodic orbits are of the form

$$\begin{aligned} x_n &= a_n \operatorname{sn}\left(\frac{2K(\kappa_n)}{\pi}\psi_n, \kappa_n\right), \\ w_n &= \sqrt{2C_n} \operatorname{cn}\left(\frac{2K(\kappa_n)}{\pi}\psi_n, \kappa_n\right) \operatorname{dn}\left(\frac{2K(\kappa_n)}{\pi}\psi_n, \kappa_n\right), \end{aligned} \quad (3.33)$$

where  $a_n = a(C_n)$ ,  $\kappa_n = \kappa(C_n)$  and

$$C_n = \Omega^{-1}\left(\frac{2\pi M}{N\varepsilon}\right) + \mathcal{O}(\varepsilon) = \Omega^{-1}\left(M\sqrt{\tilde{\gamma}}\right) + \mathcal{O}(\varepsilon). \quad (3.34)$$

This allows in particular to compute the value of the potential at the corresponding stationary point.

**Proposition 3.2.** *Let  $\varepsilon > 0$  be sufficiently small, and let  $x^\star$  be a stationary point of the potential  $V_\gamma$ , corresponding to an orbit with rotation number  $\nu = M/N$ . Then*

$$\frac{V_\gamma(x^\star)}{N} = -\frac{1}{3(1+\kappa^2)}\left[\frac{2+\kappa^2}{1+\kappa^2} - 2\frac{E(\kappa)}{K(\kappa)}\right] + \mathcal{O}(\varepsilon\kappa^2), \quad (3.35)$$

where  $\kappa = \kappa(C)$ , and  $C$  satisfies  $\Omega(C)^2 = M^2\tilde{\gamma}$ .

PROOF: The expression (2.4) for the potential implies that

$$\begin{aligned} \frac{V_\gamma(x^\star)}{N} &= \frac{1}{N} \sum_{n=1}^N \left( U(x_n) + \frac{1}{2}w_n^2 + \mathcal{O}(\varepsilon^2) \right) = \frac{1}{N} \sum_{n=1}^N (w_n^2 - C_n + \mathcal{O}(\varepsilon^2)) \\ &= \frac{C}{N} \sum_{n=1}^N \left[ 2 \operatorname{cn}^2\left(\frac{2K(\kappa)}{\pi}\psi_n, \kappa\right) \operatorname{dn}^2\left(\frac{2K(\kappa)}{\pi}\psi_n, \kappa\right) - 1 + \mathcal{O}(\varepsilon) \right] \\ &= C \left[ 2 \int_0^{2\pi} \operatorname{cn}^2\left(\frac{2K(\kappa)}{\pi}\psi, \kappa\right) \operatorname{dn}^2\left(\frac{2K(\kappa)}{\pi}\psi, \kappa\right) d\psi - 1 + \mathcal{O}(\varepsilon) \right], \end{aligned} \quad (3.36)$$

where  $C = \Omega^{-1}(M\sqrt{\tilde{\gamma}})$  and  $\kappa = \kappa(C)$ . The integral can then be computed using the change of variables  $2K(\kappa)\psi/\pi = F(\phi, \kappa)$ . Finally, recall that  $C = \kappa^2/(1 + \kappa^2)^2$ .  $\square$

One can check that  $V_\gamma(x^*)/N$  is a decreasing function of  $\kappa$ , which is itself a decreasing function of  $M^2\tilde{\gamma}$ . As a consequence,  $V_\gamma(x^*)/N$  is increasing in  $M^2\tilde{\gamma}$ . This implies in particular that the potential is larger for larger winding numbers  $M$ .

**Remark 3.3.** The leading term in the expression (3.35) for the value of the potential is the same for all orbits of a given rotation number  $\nu$ . Since stationary points of the potential of different index cannot be at exactly the same height, the difference has to be hidden in the error terms. In [BFG06a], we showed that near the desynchronisation bifurcation, the potential difference between 1-saddles and 2-saddles is of order  $(1 - \tilde{\gamma})^{N/2}$ . For large  $N$ , we expect this difference to be exponentially small in  $1/N$ , owing to the fact that near-integrable maps of a form similar to (3.22) are known to admit adiabatic invariants to that order (cf. [BK96, Theorem 2]).

### 3.4 Generating Function

In this section, we transform the problem of finding periodic orbits of the near-integrable map  $T$  into a variational problem. The fact that  $T$  is a twist map allows us to express  $I_n$  (and thus  $I_{n+1}$ ) as a function of  $\psi_n$  and  $\psi_{n+1}$ . A *generating function* of  $T$  is a function  $G(\psi_n, \psi_{n+1})$  such that

$$\partial_1 G(\psi_n, \psi_{n+1}) = -I_n, \quad \partial_2 G(\psi_n, \psi_{n+1}) = I_{n+1}. \quad (3.37)$$

It is known that any area-preserving twist map admits a generating function, unique up to an additive constant. Since  $T$  depends on the parameter  $\varepsilon$ , the generating function  $G$  naturally also depends on  $\varepsilon$ . However, we will indicate this dependence only when we want to emphasise it.

**Proposition 3.4.** *The map  $T$  admits a generating function of the form*

$$G(\psi_1, \psi_2) = \varepsilon G_0\left(\frac{\psi_2 - \psi_1}{\varepsilon}, \varepsilon\right) + 2\varepsilon^3 \sum_{p=1}^{\infty} \hat{G}_p\left(\frac{\psi_2 - \psi_1}{\varepsilon}, \varepsilon\right) \cos(p(\psi_1 + \psi_2)), \quad (3.38)$$

where the functions  $G_0(u, \varepsilon)$  and  $\hat{G}_p(u, \varepsilon)$  are real-analytic for  $u > \mathcal{O}(1/|\log \varepsilon|)$ , and satisfy

$$\begin{aligned} G'_0(u, 0) &= \bar{\Omega}^{-1}(u), \\ \hat{G}_p(u, 0) &= \frac{1}{4p\pi} \int_0^{2\pi} g(\psi, \bar{\Omega}^{-1}(u), 0) \sin(-2p\psi) \, d\psi. \end{aligned} \quad (3.39)$$

PROOF: Fix  $(\psi_2, I_2) = T(\psi_1, I_1)$ . The fact that  $T(\psi_1 + \pi, I_1) = (\psi_2 + \pi, I_2)$  implies

$$G(\psi_1 + \pi, \psi_2 + \pi) = G(\psi_1, \psi_2) + c \quad (3.40)$$

for some constant  $c$ . If we set  $G(\psi_1, \psi_2) = \tilde{G}(\psi_2 - \psi_1, \psi_1 + \psi_2)$ , we thus have

$$\tilde{G}(u, v + 2\pi) = \tilde{G}(u, v) + c. \quad (3.41)$$

This allows us to expand  $G$  as a Fourier series

$$G(\psi_1, \psi_2) = \sum_{p=-\infty}^{\infty} \tilde{G}_p(\psi_2 - \psi_1, \varepsilon) e^{ip(\psi_1 + \psi_2)} + \frac{c}{2\pi}(\psi_1 + \psi_2). \quad (3.42)$$

Next we note that the symmetry (3.23) implies  $T(-\psi_2, I_2) = (-\psi_1, I_1)$ , and thus

$$\partial_1 G(\psi_1, \psi_2) = -\partial_2 G(-\psi_2, -\psi_1) . \quad (3.43)$$

Plugging (3.42) into this relation yields

$$c = 0 \quad \text{and} \quad \tilde{G}_{-p}(u, \varepsilon) = \tilde{G}_p(u, \varepsilon) , \quad (3.44)$$

which allows to represent  $G$  as a real Fourier series as well. Computing the derivatives  $I_1 = -\partial_1 G(\psi_1, \psi_2)$  and  $I_2 = \partial_2 G(\psi_1, \psi_2)$  yields

$$I_2 - I_1 = 2 \sum_{p=-\infty}^{\infty} i p \tilde{G}_p(\psi_2 - \psi_1, \varepsilon) e^{i p (\psi_1 + \psi_2)} , \quad (3.45)$$

which shows in particular that  $\tilde{G}_p(u, \varepsilon) = \mathcal{O}(\varepsilon^3)$  for  $p \neq 0$ , as a consequence of (3.22). This implies  $I_1 = \tilde{G}'_0(\psi_2 - \psi_1, \varepsilon) + \mathcal{O}(\varepsilon^3)$ , and thus  $u = \tilde{G}'_0(\varepsilon \bar{\Omega}(u) + \mathcal{O}(\varepsilon^3), \varepsilon)$ . Renaming  $\tilde{G}_0(u, \varepsilon) = \varepsilon G_0(u/\varepsilon, \varepsilon)$  and  $\tilde{G}_p(u, \varepsilon) = \varepsilon^3 \hat{G}_p(u/\varepsilon, \varepsilon)$  yields (3.38). Evaluating (3.45) for  $\varepsilon = 0$  and taking the Fourier transform yields the expression (3.39) for  $\hat{G}_p(u, 0)$ .  $\square$

The relations (3.39) allow to determine the expression for the generating function of the map  $T$ , given by (3.22). In particular, one finds

$$G_0(u, 0) = u \bar{\Omega}^{-1}(u) - \Omega^{-1}(u) , \quad (3.46)$$

so that

$$\begin{aligned} G_0(\Omega(C), 0) &= h(C) \Omega(C) - C \\ &= -\frac{1}{3(1 + \kappa^2)} \left[ \frac{2 + \kappa^2}{1 + \kappa^2} - 2 \frac{E(\kappa)}{K(\kappa)} \right] , \end{aligned} \quad (3.47)$$

with  $\kappa = \kappa(C)$ . Note that this quantity is identical with the leading term in the expression (3.35) for the average potential per site. This indicates that we have chosen the integration constant in the generating function in such a way that  $V_\gamma$  and  $G_N$  take the same value on corresponding stationary points.

The main use of the generating function lies in the following fact. Consider the  $N$ -point function

$$G_N(\psi_1, \dots, \psi_N) = G(\psi_1, \psi_2) + G(\psi_2, \psi_3) + \dots + G(\psi_N, \psi_1 + 2\pi N\nu) , \quad (3.48)$$

defined on (a subset of) the set  $\mathbb{T}_\nu^N$ . The defining property (3.37) of the generating function implies that for any periodic orbit of period  $N$  of the map  $T$ , one has

$$\frac{\partial}{\partial \psi_n} G_N(\psi_1, \dots, \psi_N) = -I_n + I_n = 0 , \quad \text{for } n = 1, \dots, N. \quad (3.49)$$

In other words,  $N$ -periodic orbits of  $T$  with rotation number  $\nu$  are in one-to-one correspondence with stationary points of the  $N$ -point function  $G_N$  on  $\mathbb{T}_\nu^N$ .

The symmetries of the original potential imply that the  $N$ -point generating function satisfies the following relations on  $\mathbb{T}_\nu^N$ :

$$\begin{aligned} G_N(\psi_1, \dots, \psi_N) &= G_N(\psi_2, \dots, \psi_N, \psi_1 + 2\pi N\nu) , \\ G_N(\psi_1, \dots, \psi_N) &= G_N(-\psi_N, \dots, -\psi_1) , \\ G_N(\psi_1, \dots, \psi_N) &= G_N(\psi_1 + \pi, \dots, \psi_N + \pi) . \end{aligned} \quad (3.50)$$

At this point, we are in the following situation. We have first transformed the initial problem of finding the stationary points of the potential  $V_\gamma$  into the problem of finding periodic orbits of the map  $T_1$ , or, equivalently, of the map  $T$ . This problem in turn has been transformed into the problem of finding the stationary points of  $G_N$ . Obviously, the whole procedure is of interest only if the stationary points of  $G_N$  are easier to find and analyse than those of  $V_\gamma$ . This, however, is the case here since the  $N$ -point function is a small perturbation of a function depending only on the differences  $\psi_{n+1} - \psi_n$ . In other words,  $G_N$  can be interpreted as the energy of a chain of particles with a uniform nearest-neighbour interaction, put in a weak external periodic potential.

### 3.5 Fourier Representation of the Generating Function

The main difficulty in analysing the stationary points of the  $N$ -point generating function  $G_N$  comes from the fact that it is almost degenerate under translations of the form  $\psi_n \mapsto \psi_n + c \forall n$ . The purpose of this section is to decouple the translation mode from the other variables, by introducing Fourier variables.

We fix  $\nu = M/N$ . Any stationary point of  $G_N$  on  $\mathbb{T}_\nu^N$  admits a Fourier expansion of the form

$$\psi_n = 2\pi\nu n + \sum_{q=0}^{N-1} \hat{\psi}_q \omega^{qn}, \quad (3.51)$$

where  $\omega = e^{2\pi i/N}$ , and the Fourier coefficients are uniquely determined by

$$\hat{\psi}_q = \frac{1}{N} \sum_{n=1}^N \omega^{-qn} (\psi_n - 2\pi\nu n) = \overline{\hat{\psi}_{-q}}. \quad (3.52)$$

Note that  $\hat{\psi}_q = \hat{\psi}_{q+N}$  for all  $q$ . Stationary points of  $G_N$  correspond to stationary points of the function  $\overline{G}_N$ , obtained by expressing  $G_N$  in terms of Fourier variables  $(\hat{\psi}_0, \dots, \hat{\psi}_{N-1})$ . In order to do so, it is convenient to write

$$\begin{aligned} \frac{\psi_{n+1} - \psi_n}{\varepsilon} &= \Delta + \varepsilon^2 \alpha_n(\hat{\psi}_1, \dots, \hat{\psi}_{N-1}), \\ \psi_n + \psi_{n+1} &= 2\hat{\psi}_0 + 2\pi\nu(2n+1) + \varepsilon^2 \beta_n(\hat{\psi}_1, \dots, \hat{\psi}_{N-1}), \end{aligned} \quad (3.53)$$

where  $\Delta = 2\pi\nu/\varepsilon$  and

$$\begin{aligned} \alpha_n(\hat{\psi}_1, \dots, \hat{\psi}_{N-1}) &= \frac{1}{\varepsilon^3} \sum_{q=1}^{N-1} \hat{\psi}_q (\omega^q - 1) \omega^{qn}, \\ \beta_n(\hat{\psi}_1, \dots, \hat{\psi}_{N-1}) &= \frac{1}{\varepsilon^2} \sum_{q=1}^{N-1} \hat{\psi}_q (\omega^q + 1) \omega^{qn}. \end{aligned} \quad (3.54)$$

Note that  $\alpha_n$  is of order 1 in  $\varepsilon$  for any stationary point because of the expression (3.22) of the twist map. Taking the inverse Fourier transform shows that  $|\hat{\psi}_q(\omega^q - 1)| = \mathcal{O}(\varepsilon^3)$  and  $|\hat{\psi}_q| = \mathcal{O}(\varepsilon^2)$  for  $q \neq 0$ , and thus  $\beta_n$  is also of order 1.

Expressing  $G_N$  in Fourier variables yields the function

$$\overline{G}_N(\hat{\psi}_0, \dots, \hat{\psi}_{N-1}) = \sum_{p=-\infty}^{\infty} e^{2ip\hat{\psi}_0} g_p(\hat{\psi}_1, \dots, \hat{\psi}_{N-1}), \quad (3.55)$$

where (we drop the  $\varepsilon$ -dependence of  $G_0$  and  $\widehat{G}_p$ )

$$\begin{aligned} g_0(\hat{\psi}_1, \dots, \hat{\psi}_{N-1}) &= \varepsilon \sum_{n=1}^N G_0(\Delta + \varepsilon^2 \alpha_n) , \\ g_p(\hat{\psi}_1, \dots, \hat{\psi}_{N-1}) &= \varepsilon^3 \sum_{n=1}^N \widehat{G}_p(\Delta + \varepsilon^2 \alpha_n) \omega^{pM(2n+1)} e^{i\varepsilon^2 p \beta_n} \quad \text{for } p \neq 0 . \end{aligned} \quad (3.56)$$

We now examine the symmetry properties of the Fourier coefficients  $g_p$ . Table 2 shows how the Fourier variables transform under some symmetry transformations, where we only consider transformations leaving  $\mathbb{T}_\nu^N$  invariant. As a consequence, the first two symmetries in (3.50) translate into

$$\begin{aligned} g_p(\hat{\psi}_1, \dots, \hat{\psi}_{N-1}) &= \omega^{2pM} g_p(\omega \hat{\psi}_1, \dots, \omega^{N-1} \hat{\psi}_{N-1}) , \\ g_p(\hat{\psi}_1, \dots, \hat{\psi}_{N-1}) &= \omega^{-2pM} g_{-p}(-\omega^{N-1} \hat{\psi}_{N-1}, \dots, -\omega \hat{\psi}_1) . \end{aligned} \quad (3.57)$$

We now introduce new variables  $\chi_q$ ,  $q \neq 0$ , defined by

$$\chi_q = -i \omega^{-q\hat{\psi}_0/2\pi\nu} \hat{\psi}_q = -\overline{\chi_{-q}} . \quad (3.58)$$

The  $\chi_q$  are defined in such a way that they are real for stationary points satisfying, in original variables, the symmetry  $x_j = -x_{n_0-j}$  for some  $n_0$ . For later convenience, we prefer to consider  $q$  as belonging to

$$\mathcal{Q} = \left\{ -\left\lfloor \frac{N-1}{2} \right\rfloor, \dots, \left\lfloor \frac{N}{2} \right\rfloor \right\} \setminus \{0\} \quad (3.59)$$

rather than  $\{1, \dots, N-1\}$ . We set  $\chi = \{\chi_q\}_{q \in \mathcal{Q}}$  and

$$\begin{aligned} \widetilde{G}_N(\hat{\psi}_0, \chi) &= \overline{G}_N(\hat{\psi}_0, \{\hat{\psi}_q = i \omega^{q\hat{\psi}_0/2\pi\nu} \chi_q\}_{q \in \mathcal{Q}}) \\ &= \sum_{p=-\infty}^{\infty} e^{2ip\hat{\psi}_0} \tilde{g}_p(\hat{\psi}_0, \chi) , \end{aligned} \quad (3.60)$$

where

$$\tilde{g}_p(\hat{\psi}_0, \chi) = g_p(\{\hat{\psi}_q = i \omega^{q\hat{\psi}_0/2\pi\nu} \chi_q\}_{q \in \mathcal{Q}}) . \quad (3.61)$$

**Lemma 3.5.** *The function  $\widetilde{G}_N(\hat{\psi}_0, \chi)$  is  $2\pi\nu$ -periodic in its first argument.*

PROOF: By (3.57), we have

$$\tilde{g}_p(\hat{\psi}_0 + 2\pi\nu, \chi) = \omega^{-2pM} \tilde{g}_p(\hat{\psi}_0, \chi) \quad (3.62)$$

Since  $e^{2ip \cdot 2\pi\nu} = \omega^{2pM}$ , replacing  $\hat{\psi}_0$  by  $\hat{\psi}_0 + 2\pi\nu$  in (3.60) leaves  $\widetilde{G}_N$  invariant.  $\square$

$R$	$x_j \mapsto x_{j+1}$	$\psi_n \mapsto \psi_{n+1}$	$\hat{\psi}_q \mapsto \omega^q \hat{\psi}_q + 2\pi\nu \delta_{q0}$
$CS$	$x_j \mapsto -x_{N+1-j}$	$\psi_n \mapsto -\psi_{N+1-n}$	$\hat{\psi}_q \mapsto -\omega^{-q} \hat{\psi}_{N-q} - 2\pi\nu(N+1)\delta_{q0}$
$C$	$x_j \mapsto -x_j$	$\psi_n \mapsto \psi_n + \pi$	$\hat{\psi}_q \mapsto \hat{\psi}_q + \pi \delta_{q0}$

TABLE 2. Effect of some symmetries on original variables, angle variables, and Fourier variables.

Since  $\tilde{G}_N$  also has period  $\pi$ , it has in fact period

$$\frac{\pi}{N}K, \quad K = \gcd(N, 2M). \quad (3.63)$$

Our strategy now proceeds as follows:

1. Show that for each  $\hat{\psi}_0$ , and sufficiently small  $\varepsilon$ , the equations  $\partial \tilde{G}_N / \partial \chi_q = 0$ ,  $q \in \mathcal{Q}$ , admit exactly one solution  $\chi = \chi^*(\hat{\psi}_0)$ . This is done in Section 3.6 with the help of Banach's fixed-point theorem.
2. Show that for  $\chi = \chi^*(\hat{\psi}_0)$ , the equation  $\partial \tilde{G}_N / \partial \hat{\psi}_0 = 0$  is satisfied by exactly  $4N/K$  values of  $\hat{\psi}_0$ . This is done in Section 3.7 by estimating the Fourier coefficients of  $\partial \tilde{G}_N / \partial \hat{\psi}_0$  with the help of complex analysis.

### 3.6 Uniqueness of $\chi$

In this section, we show that the equations

$$\frac{\partial \tilde{G}_N}{\partial \chi_q} = 0, \quad q \in \mathcal{Q}, \quad (3.64)$$

admit exactly one solution  $\chi = \chi^*(\hat{\psi}_0)$  for each value of  $\hat{\psi}_0$ . The proof is based on a standard fixed-point argument: First we show in Lemma 3.6 that (3.64) is equivalent to the fixed-point equation  $\rho = \mathcal{T}\rho$  for a quantity  $\rho$  related to  $\chi$ . Then we show in Proposition 3.8 that  $\mathcal{T}$  is contracting in an appropriate norm, provided  $\varepsilon$  is sufficiently small.

It is useful to introduce the scaled variables

$$\rho_q = \rho_q(\chi) = -\frac{2}{\varepsilon^3} \chi_q \sin(\pi q/N) \quad (3.65)$$

and the function  $\Gamma_\ell^{(a,b)}(\rho)$ ,  $\rho = \{\rho_q\}_{q \in \mathcal{Q}}$ , defined for  $\ell \in \mathbb{Z}$  and  $a, b \geq 0$  by

$$\Gamma_\ell^{(a,b)}(\rho) = \sum_{\substack{q_1, \dots, q_a \in \mathcal{Q} \\ q'_1, \dots, q'_b \in \mathcal{Q}}} 1_{\{\sum_i q_i + \sum_j q'_j = \ell\}} \prod_{i=1}^a \rho_{q_i} \prod_{j=1}^b \frac{\varepsilon}{\tan(\pi q'_j/N)} \rho_{q'_j}. \quad (3.66)$$

By convention, any term in the sum for which  $q'_j = N/2$  for some  $j$  is zero, that is, we set  $1/\tan(\pi/2) = 0$ . A few elementary properties following immediately from this definition are:

- $\Gamma_\ell^{(0,0)}(\rho) = \delta_{\ell 0}$ ;
- $\Gamma_\ell^{(a,b)}(\rho) = 0$  for  $|\ell| > (a+b)N/2$ ;
- If  $\rho_q = 0$  for  $q \notin K\mathbb{Z}$ , then  $\Gamma_\ell^{(a,b)}(\rho) = 0$  for  $\ell \notin K\mathbb{Z}$ ;
- If  $\rho'_q = \rho_{-q}$  for all  $q$ , then  $\Gamma_\ell^{(a,b)}(\rho') = (-1)^b \Gamma_{-\ell}^{(a,b)}(\rho)$ .

The following result states that the conditions (3.64) are equivalent to a fixed-point equation.

**Lemma 3.6.** *Let*

$$H_{p,q}(\Delta) = \hat{G}_p(\Delta) - \frac{\varepsilon p \hat{G}_p(\Delta)}{\tan(\pi q/N)}, \quad (3.67)$$

with the convention that  $H_{p,N/2}(\Delta) = \widehat{G}'_p(\Delta)$ . Then the stationarity conditions (3.64) are fulfilled if and only if  $\rho = \rho(\chi)$  satisfies the fixed-point equation

$$\rho = \mathcal{T}\rho = \rho^{(0)} + \Phi(\rho, \varepsilon), \quad (3.68)$$

where the leading term is given by

$$\rho_q^{(0)} = \begin{cases} \frac{1}{G_0''(\Delta)} \sum_{k \in \mathbb{Z} : kN+q \in 2M\mathbb{Z}} (-1)^{k+1} e^{ik\hat{\psi}_0 N/M} H_{(kN+q)/2M,q}(\Delta) & \text{if } q \in K\mathbb{Z}, \\ 0 & \text{if } q \notin K\mathbb{Z}, \end{cases} \quad (3.69)$$

and the remainder is given by  $\Phi_q(\rho, \varepsilon) = \Phi_q^{(1)}(\rho, \varepsilon) + \Phi_q^{(2)}(\rho, \varepsilon)$ , with

$$\begin{aligned} \Phi_q^{(1)}(\rho, \varepsilon) &= \frac{1}{G_0''(\Delta)} \sum_{k \in \mathbb{Z}} (-1)^{k+1} e^{ik\hat{\psi}_0 N/M} \sum_{a \geq 1} \frac{\varepsilon^{2a}}{(a+1)!} G_0^{(a+2)}(\Delta) \Gamma_{kN+q}^{(a+1,0)}(\rho), \\ \Phi_q^{(2)}(\rho, \varepsilon) &= \frac{1}{G_0''(\Delta)} \sum_{k \in \mathbb{Z}} (-1)^{k+1} e^{ik\hat{\psi}_0 N/M} \sum_{a+b \geq 1} \frac{\varepsilon^{2(a+b)}}{a!b!} \sum_{p \neq 0} H_{p,q}^{(a)}(\Delta) p^b \Gamma_{kN-2pM+q}^{(a,b)}(\rho). \end{aligned} \quad (3.70)$$

The proof is a straightforward but lengthy computation, which we postpone to Appendix B.

Note the following symmetries, which follow directly from the definition of  $\rho^{(0)}$  and the properties of  $\Gamma_\ell^{(a,b)}$ :

- For all  $q \in \mathcal{Q}$ ,  $\rho_{-q}^{(0)} = \rho_q^{(0)}$ , because  $H_{-p,-q}(\Delta) = H_{p,q}(\Delta)$ , and thus  $\rho_q^{(0)} \in \mathbb{R}$ ;
- If  $\rho_q = 0$  for  $q \notin K\mathbb{Z}$ , then  $\Phi_q(\rho, \varepsilon) = 0$  for  $q \notin K\mathbb{Z}$ ;
- If  $\rho'_q = \rho_{-q}$  for all  $q$ , then  $\Phi_q(\rho', \varepsilon) = \Phi_{-q}(\rho, \varepsilon)$ ;

**Remark 3.7.** The condition  $kN + q \in 2M\mathbb{Z}$ , appearing in the definition of  $\rho^{(0)}$ , can only be fulfilled if  $q \in N\mathbb{Z} + 2M\mathbb{Z} = K\mathbb{Z}$ . If this is the case, set  $N = nK$ ,  $2M = mK$ ,  $q = \ell K$ , with  $n$  and  $m$  coprime. Then the condition becomes  $mp - kn = \ell$ . By Bezout's theorem, the general solution is given in terms of any particular solution  $(p_0, k_0)$  by

$$p = p_0 + nt, \quad k = k_0 + mt, \quad t \in \mathbb{Z}. \quad (3.71)$$

Thus there will be exactly one  $p$  with  $2|p| < n$ . If  $N$  is very large, and  $M$  is fixed, then  $n = N/K$  is also very large. Since the  $\widehat{G}_p(\Delta)$ , being Fourier coefficients of an analytic function, decrease exponentially fast in  $|p|$ , the sum in (3.69) will be dominated by the term with the lowest possible  $|p|$ .

We now introduce the following weighted norm on  $\mathbb{C}^{\mathcal{Q}}$ :

$$\|\rho\|_\lambda = \sup_{q \in \mathcal{Q}} e^{\lambda|q|/2M} |\rho_q|, \quad (3.72)$$

where  $\lambda > 0$  is a free parameter. One checks that the functions  $G_0(\Delta)$  and  $\widehat{G}_p(\Delta)$  are analytic for  $\operatorname{Re} \Delta > \mathcal{O}(1/\log|\varepsilon|)$ . Thus it follows from Cauchy's theorem that there exist positive constants  $L_0$ ,  $r < \Delta - \mathcal{O}(1/\log|\varepsilon|)$  and  $\lambda_0$  such that

$$|G_0^{(a)}(\Delta)| \leq L_0 \frac{a!}{r^a} \quad \text{and} \quad |\widehat{G}_p^{(a)}(\Delta)| \leq L_0 \frac{a!}{r^a} e^{-\lambda_0|p|} \quad (3.73)$$

for all  $a \geq 0$  and  $p \in \mathbb{Z}$ . For sufficiently small  $\varepsilon$ , it is possible to choose  $r = \Delta/2$ .

**Proposition 3.8.** *There exists a numerical constant  $c_1 > 0$  such that for any  $\Delta > 0$ , any  $\lambda < \lambda_0$  and any  $R_0 > c_1 L_0 [\Delta |G_0''(\Delta)|]^{-1}$ , there is a strictly positive  $\varepsilon_0 = \varepsilon_0(\Delta, \lambda, \lambda_0, R_0)$  such that for all  $\varepsilon < \varepsilon_0$ , the map  $\mathcal{T}$  admits a unique fixed point  $\rho^*$  in the ball  $\mathcal{B}_\lambda(0, R_0) = \{\rho \in \mathbb{C}^\mathcal{Q} : \|\rho\|_\lambda < R_0\}$ . Furthermore, the fixed point satisfies*

- $\rho_q^* = 0$  whenever  $q \notin K\mathbb{Z}$ ;
- $\rho_{-q}^* = \rho_q^*$ , and thus  $\rho_q^* \in \mathbb{R}$  for all  $q$ .

The proof is again a straightforward but lengthy computation, so we postpone it to Appendix B.

A direct consequence of this result is that for any  $\hat{\psi}_0$ , and sufficiently small  $\varepsilon$ , there is a unique  $\rho^* = \rho^*(\hat{\psi}_0)$  (and thus a unique  $\chi^*(\hat{\psi}_0)$ ) satisfying the equations  $\partial \tilde{G}_N / \partial \chi_q = 0$  for all  $q \in \mathcal{Q}$ . Indeed, we take  $R_0$  sufficiently large that our a priori estimates on the  $\chi_q$  imply that  $\rho \in \mathcal{B}_0(0, R_0)$ . Then it follows that  $\rho$  is unique. Furthermore, for any  $\lambda < \lambda_0$ , making  $\varepsilon$  sufficiently small we obtain an estimate on  $\|\rho^*\|_\lambda$ .

### 3.7 Stationary Values of $\hat{\psi}_0$

We now consider the condition  $\partial \tilde{G}_N / \partial \hat{\psi}_0 = 0$ . As pointed out at the end of Section 3.5,  $\tilde{G}_N(\hat{\psi}_0, \chi)$  is a  $\pi K/N$ -periodic function of  $\hat{\psi}_0$ . For the same reasons,  $\chi^*(\hat{\psi}_0)$  is also  $\pi K/N$ -periodic. Hence it follows that the function  $\hat{\psi}_0 \mapsto \tilde{G}_N(\hat{\psi}_0, \chi^*(\hat{\psi}_0))$  has the same period as well, and thus admits a Fourier series of the form

$$\tilde{G}_N(\hat{\psi}_0, \chi^*(\hat{\psi}_0)) = \sum_{k=-\infty}^{\infty} \hat{g}_k e^{2ik\hat{\psi}_0 N/K}, \quad (3.74)$$

with Fourier coefficients

$$\hat{g}_k = \frac{1}{2\pi} \int_0^{2\pi} \sum_{p=-\infty}^{\infty} e^{2i(p-kN/K)\hat{\psi}_0} \tilde{g}_p(\hat{\psi}_0, \chi^*(\hat{\psi}_0)) d\hat{\psi}_0 \quad (3.75)$$

(we have chosen  $[0, 2\pi]$  as interval of integration for later convenience). Using the change of variables  $\hat{\psi}_0 \mapsto -\hat{\psi}_0$  in the integral, and the various symmetries of the coefficients (in particular (3.57)), one checks that  $\hat{g}_{-k} = \hat{g}_k$ . Therefore (3.74) can be rewritten in real form as

$$\tilde{G}_N(\hat{\psi}_0, \chi^*(\hat{\psi}_0)) = \hat{g}_0 + 2 \sum_{k=1}^{\infty} \hat{g}_k \cos(2k\hat{\psi}_0 N/K). \quad (3.76)$$

Now  $\partial \tilde{G}_N / \partial \hat{\psi}_0$  vanishes if and only if the total derivative of  $\tilde{G}_N(\hat{\psi}_0, \chi^*(\hat{\psi}_0))$  with respect to  $\hat{\psi}_0$  is equal to zero. This function obviously vanishes for  $\hat{\psi}_0 = \ell\pi K/2N$ ,  $\ell = 1, \dots, 4N/K$ , and we have to show that these are the only roots.

We first observe that the Fourier coefficients  $\hat{g}_k$  can be expressed directly in terms of the generating function (3.38), written in the form

$$\tilde{G}(u, v, \varepsilon) = \varepsilon G_0(u, \varepsilon) + \varepsilon^3 \sum_{p \neq 0} \hat{G}_p(u, \varepsilon) e^{2ipv}. \quad (3.77)$$

In the sequel,  $\alpha_n^*(\hat{\psi}_0)$  and  $\beta_n^*(\hat{\psi}_0)$  denote the quantities introduced in (3.54), evaluated at  $\hat{\psi}_q = i\omega^q \hat{\psi}_0 / 2\pi\nu \chi_q^*(\hat{\psi}_0)$ .



**Lemma 3.9.** *The Fourier coefficients  $\hat{g}_k$  are given in terms of the generating function by*

$$\hat{g}_k = \frac{N}{2\pi} \int_0^{2\pi} e^{-2ik\hat{\psi}_0 N/K} \Lambda_0(\hat{\psi}_0) d\hat{\psi}_0, \quad (3.78)$$

where

$$\Lambda_0(\hat{\psi}_0) = \tilde{G}\left(\Delta + \varepsilon^2 \alpha_0^*(\hat{\psi}_0), \hat{\psi}_0 + \pi\nu + \frac{1}{2}\varepsilon^2 \beta_0^*(\hat{\psi}_0), \varepsilon\right). \quad (3.79)$$

PROOF: The coefficient  $\hat{g}_k$  can be rewritten as

$$\hat{g}_k = \frac{1}{2\pi} \sum_{n=1}^N \int_0^{2\pi} e^{-2ik\hat{\psi}_0 N/K} \Lambda_n(\hat{\psi}_0) d\hat{\psi}_0, \quad (3.80)$$

where

$$\begin{aligned} \Lambda_n(\hat{\psi}_0) &= \varepsilon G_0(\Delta + \varepsilon^2 \alpha_n^*(\hat{\psi}_0)) \\ &\quad + \varepsilon^3 \sum_{p \neq 0} p e^{2ip\hat{\psi}_0} \hat{G}_p(\Delta + \varepsilon^2 \alpha_n^*(\hat{\psi}_0)) \omega^{pM(2n+1)} e^{i\varepsilon^2 p \beta_n^*(\hat{\psi}_0)}. \end{aligned} \quad (3.81)$$

Using the periodicity of  $\chi^*$ , one finds that  $\alpha_n^*(\hat{\psi}_0 + 2\pi\nu) = \alpha_{n+1}^*(\hat{\psi}_0)$  and similarly for  $\beta_n^*$ , which implies  $\Lambda_n(\hat{\psi}_0) = \Lambda_0(\hat{\psi}_0 + 2\pi\nu n)$ . Inserting this into (3.80) and using the change of variables  $\hat{\psi}_0 \mapsto \hat{\psi}_0 - 2\pi\nu$  in the  $n$ th summand allows to express  $\hat{g}_k$  as the  $(2kN/K)$ th Fourier coefficient of  $\Lambda_0$ . Finally,  $\Lambda_0(\hat{\psi}_0)$  can also be written in the form (3.79).  $\square$

Relation (3.78) implies that the  $\hat{g}_k$  decrease exponentially fast with  $k$ , like  $e^{-2\lambda_0 k N/K}$ . Hence the Fourier series (3.76) is dominated by the first two terms, provided  $N$  is large enough. In order to obtain the existence of exactly  $4N/K$  stationary points, it is thus sufficient to prove that  $\hat{g}_1$  is also bounded below by a quantity of order  $e^{-2\lambda_0 N/K}$ .

**Proposition 3.10.** *For any  $\Delta > 0$ , there exists  $\varepsilon_1(\Delta) > 0$  such that whenever  $\varepsilon < \varepsilon_1(\Delta)$ ,*

$$\text{sign}(\hat{g}_1) = (-1)^{1+2M/K}. \quad (3.82)$$

Furthermore,

$$\frac{|\hat{g}_k|}{|\hat{g}_1|} \leq \exp\left\{-\frac{3k-5}{4}\lambda_0(\Delta)\frac{N}{K}\right\} \quad \forall k \geq 2, \quad (3.83)$$

where  $\lambda_0(\Delta)$  is a monotonously increasing function of  $\Delta$ , satisfying  $\lambda_0(\Delta) = \sqrt{2\pi}\Delta + \mathcal{O}(\Delta^2)$  as  $\Delta \searrow 0$ , and diverging logarithmically as  $\Delta \nearrow 1$ .

PROOF: First recall that  $\Delta = 2\pi\nu/\varepsilon = 2\pi M/N\varepsilon$ , where  $M$  is fixed. Thus taking  $\varepsilon$  small for given  $\Delta$  automatically yields a large  $N$ . Combining the expression (3.22) for the twist map and the defining property (3.37) of the generating function with the relations  $u = (\psi_{n+1} - \psi_n)/\varepsilon$  and  $v = \psi_n + \psi_{n+1}$ , one obtains the relation

$$\partial_v \tilde{G}(u, v, \varepsilon) = \frac{\varepsilon^3}{2} \left[ g\left(\frac{1}{2}(v - \varepsilon u), \bar{\Omega}^{-1}(u), \varepsilon\right) + \mathcal{O}(\varepsilon^2) \right]. \quad (3.84)$$

It follows from (3.24) and the definition (3.20) of  $h(C)$  that

$$\begin{aligned} g(\psi, I, 0) &= \frac{1}{\bar{\Omega}(I)} \frac{xw}{4} [1 + 2w^2 - 4x^2 + 3x^4] \\ &= \frac{1}{\bar{\Omega}(I)} \frac{xw}{4} [1 + 4C - 6x^2 + 4x^4], \end{aligned} \quad (3.85)$$

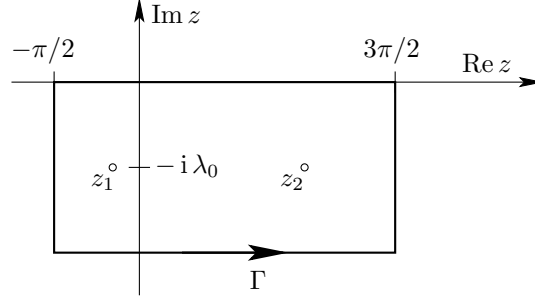


FIGURE 6. The integration contour  $\Gamma$  used in the integral (3.89).

where  $x$  and  $w$  have to be expressed as functions of  $\psi$  and  $I$  via (3.17) and (3.19). In particular, we note that

$$w = \frac{\sqrt{2C}}{a} \frac{\pi}{2K(\kappa)} \frac{dx}{d\psi} = \bar{\Omega}(I) \frac{dx}{d\psi}, \quad (3.86)$$

where we used (3.20) again. This allows us to write

$$g(\psi, I, 0) = \frac{1}{8} \frac{d}{d\psi} \left[ (1 + 4C)x^2 - 3x^4 + \frac{4}{3}x^6 \right]. \quad (3.87)$$

A similar argument would also allow to express the first-order term in  $\varepsilon$  of  $g(\psi, I, \varepsilon)$  as a function of  $x = x(\psi, I)$ . Also note the equality

$$\Delta = \bar{\Omega}(I) + \mathcal{O}(\varepsilon) = \frac{\pi b(C)}{2\sqrt{2}K(\kappa)} + \mathcal{O}(\varepsilon) = \frac{1}{\sqrt{1 + \kappa^2}K(\kappa)} + \mathcal{O}(\varepsilon), \quad (3.88)$$

which follows from the relation (3.30) between  $\nu$  and  $\bar{\Omega}(I)$ .

The properties of elliptic functions imply that for fixed  $I$ ,  $\psi \mapsto x(\psi, I)$  is periodic in the imaginary direction, with period  $2\lambda_0 = \pi K(\sqrt{1 - \kappa^2})/K(\kappa)$ , and has poles located in  $\psi = n\pi + (2m + 1)i\lambda_0$ ,  $n, m \in \mathbb{Z}$ . As a consequence, the definition of the map  $T = \Phi \circ T_2 \circ \Phi^{-1}$  implies in particular that  $g(\psi, I, \varepsilon)$  is a meromorphic function of  $\psi$ , with poles at the same location, and satisfying  $g(\psi + 2i\lambda_0, I, \varepsilon) = g(\psi, I, \varepsilon)$ . These properties yield informations on periodicity and location of poles for  $\Lambda_0(\hat{\psi}_0)$ , in particular  $\Lambda_0(\hat{\psi}_0 + 2i\lambda_0) = \Lambda_0(\hat{\psi}_0) + \mathcal{O}(\varepsilon^2)$ .

Let  $\Gamma$  be a rectangular contour with vertices in  $-\pi/2$ ,  $-\pi/2 - 2i\lambda_0$ ,  $3\pi/2 - 2i\lambda_0$ , and  $3\pi/2$ , followed in the anticlockwise direction (Figure 6), and consider the contour integral

$$J = \frac{1}{2\pi} \oint_{\Gamma} e^{-2ikzN/K} \Lambda_0(z) dz. \quad (3.89)$$

The contributions of the integrals along the vertical sides of the rectangle cancel by periodicity. Therefore, by Lemma 3.9 and the approximate periodicity of  $\Lambda_0$  in the imaginary direction,

$$J = -\frac{1}{N} \left[ \hat{g}_k - e^{-2k\lambda_0 N/K} \left( \hat{g}_k + \mathcal{O}(N\varepsilon^5) \right) \right]. \quad (3.90)$$

On the other hand, the residue theorem yields

$$J = 2\pi i \sum_{z_j} e^{-2ikz_j N/K} \text{Res}(\Lambda_0(z), z_j), \quad (3.91)$$

where the  $z_j$  denote the poles of the function  $\Lambda_0(z)$ , lying inside  $\Gamma$ . There are two such poles, located in  $z_1 = -i\lambda_0 - \pi\nu + \varepsilon\Delta + \mathcal{O}(\varepsilon^2)$ , and  $z_2 = z_1 + \pi$ , and they both yield the same contribution, of order  $e^{-\lambda_0 k N(1 + \mathcal{O}(\varepsilon^2))/K}$ , to the sum. Comparing (3.90) and (3.91) shows that  $\hat{g}_k/N$  is of the same order. Finally, the leading term of  $\hat{g}_1$  can be determined explicitly using (3.87) and Jacobi's expression (A.11) for the Fourier coefficients of powers of elliptic functions, and is found to have sign  $(-1)^{1+2M/K}$  for sufficiently large  $N$ . Choosing  $\varepsilon$  small enough (for fixed  $\varepsilon N$ ) guarantees that  $\hat{g}_1$  dominates all  $\hat{g}_k$  for  $k \geq 2$ .  $\square$

**Corollary 3.11.** *For  $\varepsilon < \varepsilon_1(\Delta)$ , the  $N$ -point generating function  $\tilde{G}_N$  admits exactly  $4N/K$  stationary points, given by  $\hat{\psi}_0 = \ell\pi K/2N$ ,  $\ell = 1, \dots, 4N/K$ , and  $\chi = \chi^*(\hat{\psi}_0)$ .*

PROOF: In the points  $\hat{\psi}_0 = \ell\pi K/2N$ , the derivative of the function  $\hat{\psi}_0 \mapsto \tilde{G}_N(\hat{\psi}_0, \chi^*(\hat{\psi}_0))$  vanishes, while its second derivative is bounded away from zero, as a consequence of Estimate (3.83). Thus these points are simple roots of the first derivative, which is bounded away from zero everywhere else.  $\square$

### 3.8 Index of the Stationary Points

We finally examine the stability type of the various stationary points, by first determining their index as stationary points of the  $N$ -point generating function  $\tilde{G}_N$ , and then examining how this translates into their index as stationary points of the potential  $V_\gamma$ .

**Proposition 3.12.** *Let  $(\hat{\psi}_0, \chi^*(\hat{\psi}_0))$  be a stationary point of  $\tilde{G}_N$  with rotation number  $\nu = N/M$ . Let  $x^* = x^*(\hat{\psi}_0)$  be the corresponding stationary point of the potential  $V_\gamma$ , and let  $K = \gcd(N, 2M)$ .*

- *If  $2M/K$  is odd, then the points  $x^*(0)$ ,  $x^*(K\pi/N)$ ,  $\dots$  are saddles of even index of  $V_\gamma$ , while the points  $x^*(K\pi/2N)$ ,  $x^*(3K\pi/2N)$ ,  $\dots$  are saddles of odd index of  $V_\gamma$ .*
- *If  $2M/K$  is even, then the points  $x^*(0)$ ,  $x^*(K\pi/N)$ ,  $\dots$  are saddles of odd index of  $V_\gamma$ , while the points  $x^*(K\pi/2N)$ ,  $x^*(3K\pi/2N)$ ,  $\dots$  are saddles of even index of  $V_\gamma$ .*

PROOF: We first determine the index of  $(\hat{\psi}_0, \chi^*(\hat{\psi}_0))$  as stationary point of  $\tilde{G}_N$ . Using the fact that  $G''_0(\Delta)$  is negative ( $\bar{\Omega}^{-1}(\Delta)$  being decreasing), one sees that the Hessian matrix of  $\tilde{G}_N$  is a small perturbation of a diagonal matrix with  $N - 1$  negative eigenvalues. The  $N$ th eigenvalue, which corresponds to translations of  $\hat{\psi}_0$ , has the same sign as the second derivative of  $\hat{\psi}_0 \mapsto \tilde{G}_N(\hat{\psi}_0, \chi^*(\hat{\psi}_0))$ , which is equal to  $(-1)^{2M/K} \text{sign} \cos(2\hat{\psi}_0 N/K)$ . Thus  $(\hat{\psi}_0, \chi^*(\hat{\psi}_0))$  is an  $N$ -saddle of  $\tilde{G}_N$  if this sign is negative, and an  $(N - 1)$ -saddle otherwise. The same is true for the index of  $\psi = (\psi_1, \dots, \psi_N)$  as a stationary point of  $\tilde{G}_N$ .

Let  $R$  be the so-called *residue* of the periodic orbit of  $T$  associated with the stationary point. This residue is equal to  $(2 - \text{Tr}(DT^N))/4$ , where  $DT^N$  is the Jacobian of  $T^N$  at the orbit, and indicates the stability type of the periodic orbit: The orbit is hyperbolic if  $R < 0$ , elliptic if  $0 < R < 1$ , and inverse hyperbolic if  $R > 1$ . It is known [MM83] that the residue  $R$  is related to the index of  $\psi$  by the identity

$$R = -\frac{1}{4} \frac{\det(\text{Hess } \tilde{G}_N(\psi))}{\prod_{j=1}^N (-\partial_{12} G(\psi_j, \psi_{j+1}))}. \quad (3.92)$$

In our case,  $-\partial_{12} G(\psi_j, \psi_{j+1})$  is always negative, so that  $R$  is positive if  $\psi$  is an  $(N - 1)$ -saddle, and negative if  $\psi$  is an  $N$ -saddle.

Now  $x^*(\hat{\psi}_0)$  also corresponds to a periodic orbit of the map (3.2), whose generating function is  $H(x_n, x_{n+1}) = \frac{1}{2}(x_n - x_{n+1})^2 + \frac{2}{\gamma}U(x_n)$ . The corresponding  $N$ -point generating

function is precisely  $(2/\gamma)V_\gamma$ . Since the residue is invariant under area-preserving changes of variables, we also have

$$R = -\frac{1}{2\gamma} \frac{\det(\text{Hess } V_\gamma(x^*))}{\prod_{j=1}^N (-\partial_{12} H(x_j^*, x_{j+1}^*))} . \quad (3.93)$$

In this case, the denominator is positive. Therefore,  $\text{Hess } V_\gamma(x^*)$  has an even number of positive eigenvalues if  $\psi$  is an  $N$ -saddle, and an odd number of positive eigenvalues if  $\psi$  is an  $(N-1)$ -saddle.  $\square$

We can now complete the proofs of Theorem 2.1 and Theorem 2.2.

PROOF OF THEOREM 2.1. We first recall the following facts, established in [BFG06a]. Whenever  $\tilde{\gamma}$  crosses a bifurcation value  $\tilde{\gamma}_M$ , say from larger to smaller values, the index of the origin changes from  $2M-1$  to  $2M+1$ . Thus the bifurcation involves a centre manifold of dimension 2, with  $2M-1$  unstable and  $N-2M-1$  stable directions transversal to the manifold. Within the centre manifold, the origin repels nearby trajectories, and attracts trajectories starting sufficiently far away. Therefore, all stationary points lying in the centre manifold, except the origin, are either sinks or saddles for the reduced two-dimensional dynamics. For the full dynamics, they are thus saddles of index  $(2M-1)$  or  $2M$  (c.f. [BFG06a, Section 4.3]), at least for  $\tilde{\gamma}$  close to  $\tilde{\gamma}_M$ .

We now return to the twist map in action-angle variables (3.22). The frequency  $\bar{\Omega}(I)$  being maximal for  $I=0$ , as  $\varepsilon$  increases, new orbits appear on the line  $I=0$ , which corresponds to the origin in  $x$ -coordinates. Orbits of rotation number  $\nu = M/N$  can only exist if  $\varepsilon \bar{\Omega}(0) = \varepsilon \geq 2\pi\nu + \mathcal{O}(\varepsilon^2)$ , which is compatible with the condition  $\tilde{\gamma} < \tilde{\gamma}_M$ .

Consider the case of a winding number  $M=1$ , that is, of orbits with rotation number  $\nu = 1/N$ , which are the only orbits existing for  $\tilde{\gamma}_2 < \tilde{\gamma} < \tilde{\gamma}_1$ . We note that  $\tilde{\gamma} > \tilde{\gamma}_2$  implies  $\Delta = 2\pi/N\varepsilon > 1/2 - \mathcal{O}(\varepsilon)$ , and thus there exists  $N_1 < \infty$  such that the condition  $N \geq N_1$  automatically implies that  $\varepsilon$  is small enough for Corollary 3.11 to hold. Now, Proposition 3.12 yields:

- If  $N$  is even, then  $K = \gcd(N, 2) = 2$ , and there are  $2N$  stationary points. The points  $x^*(0), x^*(2\pi/N), \dots$  must be 2-saddles, while the points  $x^*(\pi/N), x^*(3\pi/N), \dots$  are 1-saddles;
- If  $N$  is odd, then  $K = \gcd(N, 2) = 1$ , and there are  $4N$  stationary points. The points  $x^*(0), x^*(\pi/N), \dots$  must be 1-saddles, while the points  $x^*(\pi/2N), x^*(3\pi/2N), \dots$  are 2-saddles.

Going back to original variables, we obtain the expressions (2.30) and (2.31) for the coordinates of these stationary points. The fact that they keep the same index as  $\tilde{\gamma}$  moves away from  $\tilde{\gamma}_M$  is a consequence of Relation (3.93) and the fact that the corresponding stationary points of  $\tilde{G}_N$  also keep the same index. Finally, Relation (2.26) on the potential difference is a consequence of Proposition 3.2. This proves Theorem 2.1.  $\square$

PROOF OF THEOREM 2.2. For larger winding number  $M$ , one can proceed in an analogous way, provided  $N$  is sufficiently large, as a function of  $M$ , for the conditions on  $\varepsilon$  to hold. This proves Theorem 2.2.  $\square$

Finally, Theorem 2.4 is proved in an analogous way as Theorems 2.7 and 2.8 in [BFG06a], using results from [FW98] (see also [Kif81, Sug96]).

## A Jacobi's Elliptic Integrals and Functions

Fix some  $\kappa \in [0, 1]$ . The *incomplete elliptic integrals of the first and second kind* are defined, respectively, by<sup>3</sup>

$$F(\phi, \kappa) = \int_0^\phi \frac{dt}{\sqrt{1 - \kappa^2 \sin^2 t}}, \quad E(\phi, \kappa) = \int_0^\phi \sqrt{1 - \kappa^2 \sin^2 t} dt. \quad (\text{A.1})$$

The *complete elliptic integrals of the first and second kind* are given by

$$K(\kappa) = F(\pi/2, \kappa), \quad E(\kappa) = E(\pi/2, \kappa). \quad (\text{A.2})$$

Special values include  $K(0) = E(0) = \pi/2$  and  $E(1) = 1$ . The integral of the first kind  $K(\kappa)$  diverges logarithmically as  $\kappa \nearrow 1$ .

The *Jacobi amplitude*  $\text{am}(u, \kappa)$  is the inverse function of  $F(\cdot, \kappa)$ , i.e.,

$$\phi = \text{am}(u, \kappa) \Leftrightarrow u = F(\phi, \kappa). \quad (\text{A.3})$$

The three standard Jacobi elliptic functions are then defined as

$$\begin{aligned} \text{sn}(u, \kappa) &= \sin(\text{am}(u, \kappa)), \\ \text{cn}(u, \kappa) &= \cos(\text{am}(u, \kappa)), \\ \text{dn}(u, \kappa) &= \sqrt{1 - \kappa^2 \sin^2(\text{am}(u, \kappa))}. \end{aligned} \quad (\text{A.4})$$

Their derivatives are given by

$$\begin{aligned} \text{sn}'(u, \kappa) &= \text{cn}(u, \kappa) \text{dn}(u, \kappa), \\ \text{cn}'(u, \kappa) &= -\text{sn}(u, \kappa) \text{dn}(u, \kappa), \\ \text{dn}'(u, \kappa) &= -\kappa^2 \text{sn}(u, \kappa) \text{cn}(u, \kappa). \end{aligned} \quad (\text{A.5})$$

The function  $\text{sn}$  satisfies the periodicity relations

$$\begin{aligned} \text{sn}(u + 4K(\kappa), \kappa) &= \text{sn}(u, \kappa), \\ \text{sn}(u + 2iK(\sqrt{1 - \kappa^2}), \kappa) &= \text{sn}(u, \kappa), \end{aligned} \quad (\text{A.6})$$

and has simple poles in  $u = 2nK(\kappa) + (2m + 1)iK(\sqrt{1 - \kappa^2})$ ,  $n, m \in \mathbb{Z}$ , with residue  $(-1)^m/\kappa$ . The functions  $\text{cn}$  and  $\text{dn}$  satisfy similar relations. Since  $\text{am}(u, 0) = u$ , one has  $\text{sn}(u, 0) = \sin u$ ,  $\text{cn}(u, 0) = \cos u$  and  $\text{dn}(u, 0) = 1$ . As  $\kappa$  grows from 0 to 1, the elliptic functions become more and more squarish. This is also apparent from their Fourier series, given by

$$\begin{aligned} \frac{2K(\kappa)}{\pi} \text{sn}\left(\frac{2K(\kappa)}{\pi}\psi, \kappa\right) &= \frac{4}{\kappa} \sum_{p=0}^{\infty} \frac{q^{(2p+1)/2}}{1 - q^{2p+1}} \sin((2p+1)\psi), \\ \frac{2K(\kappa)}{\pi} \text{cn}\left(\frac{2K(\kappa)}{\pi}\psi, \kappa\right) &= \frac{4}{\kappa} \sum_{p=0}^{\infty} \frac{q^{(2p+1)/2}}{1 + q^{2p+1}} \cos((2p+1)\psi), \\ \frac{2K(\kappa)}{\pi} \text{dn}\left(\frac{2K(\kappa)}{\pi}\psi, \kappa\right) &= 1 + 4 \sum_{p=0}^{\infty} \frac{q^p}{1 + q^{2p}} \cos(2p\psi), \end{aligned} \quad (\text{A.7})$$

---

<sup>3</sup>One should beware of the fact that some sources use  $m = \kappa^2$  as parameter.

where  $q = q(\kappa)$  is the *elliptic nome* defined by

$$q = \exp \left\{ -\pi \frac{K(\sqrt{1-\kappa^2})}{K(\kappa)} \right\}. \quad (\text{A.8})$$

The elliptic nome has the asymptotic behaviour

$$q(\kappa) = \begin{cases} \frac{\kappa^2}{16} + \frac{\kappa^4}{32} + \mathcal{O}(\kappa^6) & \text{for } \kappa \searrow 0, \\ \exp \left\{ \frac{\pi^2}{\log[(1-\kappa^2)/16]} \right\} \left[ 1 + \mathcal{O} \left( \frac{1-\kappa^2}{\log^2[(1-\kappa^2)/16]} \right) \right] & \text{for } \kappa \nearrow 1. \end{cases} \quad (\text{A.9})$$

We also use the following identities, derived in [Jac69, p. 175]. For  $k \geq 1$ ,

$$\left( \frac{2K(\kappa)}{\pi} \right)^{2k} \text{sn}^{2k} \left( \frac{2K(\kappa)}{\pi} \psi, \kappa \right) = \hat{c}_{2k,0} + \sum_{p=1}^{\infty} \hat{c}_{2k,p} \frac{q^p}{1-q^{2p}} \cos(2p\psi), \quad (\text{A.10})$$

where the  $\hat{c}_{2k,0}$  are positive constants (independent of  $\psi$ ), and the other Fourier coefficients are given for the first few  $k$  by

$$\begin{aligned} \hat{c}_{2,p} &= -\frac{4}{\kappa^2} (2p), \\ \hat{c}_{4,p} &= \frac{4}{3!\kappa^4} \left[ (2p)^3 - 4(2p)(1+\kappa^2) \left( \frac{2K(\kappa)}{\pi} \right)^2 \right], \\ \hat{c}_{6,p} &= -\frac{4}{5!\kappa^6} \left[ (2p)^5 - 20(2p)^3(1+\kappa^2) \left( \frac{2K(\kappa)}{\pi} \right)^2 + 8(2p)(8+7\kappa^2+8\kappa^4) \left( \frac{2K(\kappa)}{\pi} \right)^4 \right]. \end{aligned} \quad (\text{A.11})$$

## B Proofs of the Fixed-Point Argument

In this appendix, we give the somewhat technical proofs of the fixed-point argument given in Section 3.6. We start by proving Lemma 3.6, stating a fixed-point equation equivalent to the stationarity conditions  $\partial \tilde{G}_N / \partial \chi_q = 0$ ,  $q \in \mathcal{Q}$ .

PROOF OF LEMMA 3.6. The definitions (3.54) of  $\alpha_n$  and  $\beta_n$  imply, for any  $a, b \geq 0$ ,

$$\begin{aligned} \alpha_n^a &= \sum_{q_1, \dots, q_a \in \mathcal{Q}} \prod_{i=1}^a \rho_{q_i} \omega^{q_i(n+1/2)} e^{i\hat{\psi}_0 q_i/M}, \\ \beta_n^b &= \sum_{q'_1, \dots, q'_b \in \mathcal{Q}} \prod_{j=1}^b \frac{-i\varepsilon \rho_{q'_j}}{\tan(\pi q'_j/N)} \omega^{q'_j(n+1/2)} e^{i\hat{\psi}_0 q'_j/M}. \end{aligned} \quad (\text{B.1})$$

It is more convenient to compute  $\partial \tilde{G}_N / \partial \rho_{-q}$  rather than  $\partial \tilde{G}_N / \partial \chi_q$ . We thus have to compute the derivatives of  $\tilde{g}_p$  with respect to  $\rho_{-q}$  for all  $p$ . For  $p = 0$ , we have

$$\frac{\partial \tilde{g}_0}{\partial \rho_{-q}} = \varepsilon^3 \sum_{n=1}^N G'_0(\Delta + \varepsilon^2 \alpha_n) \frac{\partial \alpha_n}{\partial \rho_{-q}}, \quad (\text{B.2})$$

where (B.1) shows that  $\partial\alpha_n/\partial\rho_{-q} = \omega^{-q(n+1/2)} e^{-i\hat{\psi}_0 q/M}$ . We expand  $G'_0(\Delta + \varepsilon^2\alpha_n)$  into powers of  $\varepsilon^2$ , and plug in (B.1) again. In the resulting expression, the sum over  $n$  vanishes unless  $\sum_i q_i - q$  is a multiple of  $N$ , say  $kN$ . This yields

$$\frac{\partial\tilde{g}_0}{\partial\rho_{-q}} = N\varepsilon^3 \sum_{k \in \mathbb{Z}} (-1)^k e^{ik\hat{\psi}_0 N/M} \sum_{a \geq 0} \frac{\varepsilon^{2a}}{a!} G_0^{(a+1)}(\Delta) \Gamma_{kN+q}^{(a,0)}(\rho). \quad (\text{B.3})$$

We consider the terms  $a = 0$  and  $a = 1$  separately:

- Since  $\Gamma_{kN+q}^{(0,0)}(\rho) = \delta_{kN,-q}$  vanishes for all  $k$ , the sum actually starts at  $a = 1$ .
- The fact that  $\Gamma_\ell^{(1,0)}(\rho)$  vanishes whenever  $|\ell| > N/2$  implies that only the term  $k = 0$  contributes, and yields a contribution proportional to  $-\rho_q$ .

Shifting the summation index  $a$  by one unit, we get

$$\frac{\partial\tilde{g}_0}{\partial\rho_{-q}} = N\varepsilon^5 \left[ G_0''(\Delta) \rho_q + \sum_{k \in \mathbb{Z}} (-1)^k e^{ik\hat{\psi}_0 N/M} \sum_{a \geq 1} \frac{\varepsilon^{2a}}{(a+1)!} G_0^{(a+2)}(\Delta) \Gamma_{kN+q}^{(a+1,0)}(\rho) \right]. \quad (\text{B.4})$$

A similar computation for  $p \neq 0$  shows that

$$\frac{\partial\tilde{g}_p}{\partial\rho_{-q}} e^{2ip\hat{\psi}_0} = N\varepsilon^5 \sum_{k \in \mathbb{Z}} (-1)^k e^{ik\hat{\psi}_0 N/M} \sum_{a,b \geq 0} \frac{\varepsilon^{2(a+b)}}{a!b!} H_{p,q}^{(a)}(\Delta) p^b \Gamma_{kN+q-2pM}^{(a,b)}. \quad (\text{B.5})$$

Solving the stationarity condition

$$0 = \frac{\partial\tilde{G}_N}{\partial\rho_{-q}} = \sum_{p=-\infty}^{\infty} e^{2ip\hat{\psi}_0} \frac{\partial\tilde{g}_p}{\partial\rho_{-q}} \quad (\text{B.6})$$

with respect to  $\rho_q$ , and singling out the term  $a = b = 0$  in (B.5) to give the leading term  $\rho^{(0)}$  then yields the result.  $\square$

The following estimates yield sufficient conditions for the operator  $\mathcal{T}$  to be a contraction inside a certain ball, for the norm  $\|\cdot\|_\lambda$  introduced in (3.72).

**Proposition B.1.** *There exist numerical constants  $c_0, c_1 > 0$ , such that for any  $\lambda < \lambda_0$ , and any  $N$  such that  $N e^{-\lambda_0 N/2M} \leq 1/2$ , the estimates*

$$\|\mathcal{T}\rho\|_\lambda \leq \frac{c_1 L_0}{\Delta |G_0''(\Delta)|} \left[ 1 + \frac{M}{\Delta^3} \left( \|\rho\|_\lambda + \varepsilon \Delta M \eta(\lambda_0, \lambda) \right) \varepsilon \|\rho\|_\lambda \right], \quad (\text{B.7})$$

$$\|\mathcal{T}\rho - \mathcal{T}\rho'\|_\lambda \leq \frac{c_1 L_0}{|G_0''(\Delta)|} \frac{M}{\Delta^4} \left[ (\|\rho\|_\lambda \vee \|\rho'\|_\lambda) + \varepsilon \Delta M \eta(\lambda_0, \lambda) \right] \varepsilon \|\rho - \rho'\|_\lambda \quad (\text{B.8})$$

hold with  $\eta(\lambda_0, \lambda) = (e^\lambda / \lambda_0) \vee (1/(\lambda_0 - \lambda))$ , provided  $\rho$  and  $\rho'$  satisfy

$$\varepsilon (\|\rho\|_\lambda \vee \|\rho'\|_\lambda) \leq c_0 \frac{\Delta^2}{M} \left( 1 \wedge \frac{\lambda_0 - \lambda}{M} \wedge \frac{\lambda}{M} \right). \quad (\text{B.9})$$

PROOF: The lower bound

$$\frac{|\tan(\pi q/N)|}{\varepsilon} \geq \frac{\pi|q|}{N\varepsilon} = \frac{\Delta}{2M}|q| \quad (\text{B.10})$$

directly implies

$$|H_{p,q}^{(a)}(\Delta)| \leq L_0 \frac{a!}{r^{a+1}} \left[ 1 + \frac{2M|p|}{|q|} \right] e^{-\lambda_0|p|} . \quad (\text{B.11})$$

The assumption on  $N$  allows  $|\rho_q|$  to be bounded by a geometric series of ratio smaller than  $1/2$ , which is dominated by the term  $k = 0$ , yielding

$$\|\rho^{(0)}\|_\lambda \leq \frac{c_2 L_0}{\Delta |G_0''(\Delta)|} e^{-(\lambda_0 - \lambda)|q|/2M} \leq \frac{c_2 L_0}{\Delta |G_0''(\Delta)|} , \quad (\text{B.12})$$

where  $c_2 > 0$  is a numerical constant. The fact that  $\Gamma_\ell^{(a,b)}(\rho)$  contains less than  $N^{a+b-1}$  terms, together with (B.10), implies the bound

$$|\Gamma_\ell^{(a,b)}(\rho)| \leq N^{a+b-1} \left( \frac{2M}{\Delta} \right)^b e^{-\lambda|\ell|/2M} \|\rho\|_\lambda^{a+b} . \quad (\text{B.13})$$

Assuming that  $\|\rho\|_\lambda \leq c_0 \Delta^2 / M \varepsilon$  for sufficiently small  $c_0$ , it is straightforward to obtain the estimate

$$\|\Phi^{(1)}(\rho, \varepsilon)\|_\lambda \leq \frac{c_3 L_0}{|G_0''(\Delta)|} \frac{2M}{\Delta^4} \varepsilon \|\rho\|_\lambda^2 . \quad (\text{B.14})$$

In the sequel, we assume that  $q > 0$ , since by symmetry of the norm under permutation of  $\rho_q$  and  $\rho_{-q}$  the same estimates will hold for  $q < 0$ . The norm of  $\Phi^{(2)}(\rho, \varepsilon)$  is more delicate to estimate. We start by writing

$$|\Phi_q^{(2)}(\rho, \varepsilon)| \leq \frac{L_0}{|G_0''(\Delta)|} \frac{1}{N} \sum_{a+b \geq 1} (\varepsilon^2 N \|\rho\|_\lambda)^{a+b} \frac{1}{r^{a+1}} \left( \frac{2M}{\Delta} \right)^b S_q(b) , \quad (\text{B.15})$$

where

$$S_q(b) = \frac{1}{b!} \sum_{p \neq 0} |p|^b \left( 1 + \frac{2M|p|}{q} \right) e^{-(\lambda_0 - \lambda)|p|} \sum_{k \in \mathbb{Z}} \exp \left\{ -\frac{\lambda}{2M} (2M|p| + |kN + q - 2Mp|) \right\} . \quad (\text{B.16})$$

We decompose  $S_q(b) = S_q^+(b) + S_q^-(b)$ , where  $S_q^+(b)$  and  $S_q^-(b)$  contain, respectively, the sum over positive and negative  $p$ . In the sequel, we shall only treat the term  $S_q^+(b)$ . The sum over  $k$  in (B.16) is dominated by the term for which  $kN$  is the closest possible to  $2Mp - q$ , and can be bounded by a geometric series. The result for  $p > 0$  is

$$\sum_{k \in \mathbb{Z}} \exp \left\{ -\frac{\lambda}{2M} (2Mp + |kN + q - 2Mp|) \right\} \leq c_4 (e^{-\lambda p} \wedge e^{-\lambda q/2M}) . \quad (\text{B.17})$$

We now distinguish between two cases.

- If  $q \leq 2M$ , we bound the sum over  $k$  by  $e^{-\lambda p}$ , yielding

$$S_q^+(b) \leq \frac{c_4}{b!} \frac{4M}{q} \sum_{p \geq 1} p^{b+1} e^{-\lambda_0 p} \leq 4M c_5 \frac{b+1}{\lambda_0^b} . \quad (\text{B.18})$$

Since  $e^{\lambda q/2M} \leq e^\lambda$ , it follows that

$$|\Phi_q^{(2)}(\rho, \varepsilon)| \leq \frac{c_6 L_0}{|G_0''(\Delta)|} \frac{2M^2 e^\lambda}{r^2 \Delta \lambda_0} \varepsilon^2 \|\rho\|_\lambda e^{-\lambda q/2M} . \quad (\text{B.19})$$



- If  $q > 2M$ , we split the sum over  $p$  at  $q/2M$ . For  $2Mp \leq q$ , we bound  $(1 + 2Mp/q)$  by 2 and the sum over  $k$  by  $e^{-\lambda q/2M}$ . For  $2Mp > q$ , we bound the the sum over  $k$  by  $e^{-\lambda p} \leq e^{-\lambda q/2M}$ . This shows

$$S_q^+(b) \leq 2c_7 M \frac{b+1}{(\lambda_0 - \lambda)^b} e^{-\lambda q/2M}, \quad (\text{B.20})$$

and thus

$$|\Phi_q^{(2)}(\rho, \varepsilon)| \leq \frac{c_8 L_0}{|G_0''(\Delta)|} \frac{2M^2}{r^2 \Delta (\lambda_0 - \lambda)} \varepsilon^2 \|\rho\|_\lambda e^{-\lambda q/2M}. \quad (\text{B.21})$$

Now (B.21) and (B.19), together with (B.12), imply (B.7). The proof of (B.8) is similar, showing first the estimate

$$\left| \prod_{i=1}^a \rho_{q_i} - \prod_{i=1}^a \rho'_{q_i} \right| \leq a (\|\rho\|_\lambda \vee \|\rho'\|_\lambda)^{a-1} e^{-\lambda \sum_{i=1}^a |q_i|/2M} \|\rho - \rho'\|_\lambda \quad (\text{B.22})$$

by induction on  $a$ , and then

$$|\Gamma_\ell^{(a,b)}(\rho) - \Gamma_\ell^{(a,b)}(\rho')| \leq (a+b) [N(\|\rho\|_\lambda \vee \|\rho'\|_\lambda)]^{a+b-1} \left( \frac{2M}{\Delta} \right)^b e^{-\lambda |\ell|/2M} \|\rho - \rho'\|_\lambda. \quad (\text{B.23})$$

□

It is now easy to complete the proof of Proposition 3.8.

PROOF OF PROPOSITION 3.8. Estimate (B.7) for  $\|\mathcal{T}\rho\|_\lambda$  implies that if

$$\varepsilon \leq \frac{R_0}{\Delta M \eta(\lambda_0, \lambda)} \wedge \frac{\Delta^3}{2MR_0^2} \left( \frac{\Delta |G_0''(\Delta)|}{c_1 L_0} R_0 - 1 \right), \quad (\text{B.24})$$

then  $\mathcal{T}(\mathcal{B}_\lambda(0, R_0)) \subset \mathcal{B}_\lambda(0, R_0)$ . If in addition

$$\varepsilon \leq c_0 \frac{\Delta^2}{MR_0} \left( 1 \wedge \frac{\lambda_0 - \lambda}{M} \wedge \frac{\lambda}{M} \right), \quad (\text{B.25})$$

then Estimate (B.8) for  $\|\mathcal{T}\rho - \mathcal{T}\rho'\|_\lambda$  applies for  $\rho, \rho' \in \mathcal{B}_\lambda(0, R_0)$ . It is then immediate to check that  $\mathcal{T}$  is a contracting in  $\mathcal{B}_\lambda(0, R_0)$ , as a consequence of (B.24). Thus the existence of a unique fixed point in that ball follows by Banach's contraction lemma. Finally, the assertions on the properties of  $\rho^*$  follow from the facts that they are true for  $\rho^{(0)}$ , that they are preserved by  $\mathcal{T}$  and that  $\rho^* = \lim_{n \rightarrow \infty} \mathcal{T}^n \rho^{(0)}$ . □

## References

- [BFG06a] Nils Berglund, Bastien Fernandez, and Barbara Gentz, *Metastability in interacting non-linear stochastic differential equations I: From weak coupling to synchronisation*, Preprint, 2006.
- [BHP05] D. Blömker, M. Hairer, and G. A. Pavliotis, *Modulation equations: stochastic bifurcation in large domains*, Comm. Math. Phys. **258** (2005), no. 2, 479–512.
- [BK96] Nils Berglund and Hervé Kunz, *Integrability and ergodicity of classical billiards in a magnetic field*, J. Statist. Phys. **83** (1996), no. 1-2, 81–126.
- [dH04] F. den Hollander, *Metastability under stochastic dynamics*, Stochastic Process. Appl. **114** (2004), no. 1, 1–26.
- [EH01] J.-P. Eckmann and M. Hairer, *Uniqueness of the invariant measure for a stochastic PDE driven by degenerate noise*, Comm. Math. Phys. **219** (2001), no. 3, 523–565.
- [FW98] M. I. Freidlin and A. D. Wentzell, *Random perturbations of dynamical systems*, second ed., Springer-Verlag, New York, 1998.
- [Jac69] C. G. J. Jacobi, *Fundamenta nova theoriae functionum ellipticarum. Regimonti. Sumptibus fratrum Bornträger 1829*, Gesammelte Werke, Vol. 1, Chelsea Publishing Company, New York, 1969, pp. 49–239.
- [Kif81] Yuri Kifer, *The exit problem for small random perturbations of dynamical systems with a hyperbolic fixed point*, Israel J. Math. **40** (1981), no. 1, 74–96.
- [Mei92] J. D. Meiss, *Symplectic maps, variational principles, and transport*, Rev. Modern Phys. **64** (1992), no. 3, 795–848.
- [MM83] R. S. MacKay and J. D. Meiss, *Linear stability of periodic orbits in Lagrangian systems*, Phys. Lett. A **98** (1983), no. 3, 92–94.
- [OV05] Enzo Olivieri and Maria Eulália Vares, *Large deviations and metastability*, Encyclopedia of Mathematics and its Applications, vol. 100, Cambridge University Press, Cambridge, 2005.
- [Rou02] Jacques Rougemont, *Space-time invariant measures, entropy, and dimension for stochastic Ginzburg-Landau equations*, Comm. Math. Phys. **225** (2002), no. 2, 423–448.
- [Sug96] Makoto Sugiura, *Exponential asymptotics in the small parameter exit problem*, Nagoya Math. J. **144** (1996), 137–154.

Nils Berglund  
CPT–CNRS LUMINY  
Case 907, 13288 Marseille Cedex 9, France  
*and*  
PHYMAT, UNIVERSITÉ DU SUD TOULON–VAR  
*Present address:*  
MAPMO–CNRS, UNIVERSITÉ D’ORLÉANS  
Bâtiment de Mathématiques, Rue de Chartres  
B.P. 6759, 45067 Orléans Cedex 2, France  
*E-mail address:* `berglund@cpt.univ-mrs.fr`

Bastien Fernandez  
CPT–CNRS LUMINY  
Case 907, 13288 Marseille Cedex 9, France  
*E-mail address:* `fernandez@cpt.univ-mrs.fr`

Barbara Gentz  
WEIERSTRASS INSTITUTE FOR APPLIED ANALYSIS AND STOCHASTICS  
Mohrenstraße 39, 10117 Berlin, Germany  
*Present address:*  
FACULTY OF MATHEMATICS, UNIVERSITY OF BIELEFELD  
P.O. Box 10 01 31, 33501 Bielefeld, Germany  
*E-mail address:* `gentz@math.uni-bielefeld.de`